Exploring Ancestry-Related Differences in Dengue Virus Infection in Human Skin

by

Jocelyn M. Taddonio

B.S. in General Biology, University of Maryland, 2021

B.A. in Criminology and Criminal Justice, University of Maryland, 2021

Submitted to the Graduate Faculty of the

School of Public Health in partial fulfillment

of the requirements for the degree of

Master of Science

University of Pittsburgh

2024

UNIVERSITY OF PITTSBURGH

SCHOOL OF PUBLIC HEALTH

This thesis was presented

by

Jocelyn M. Taddonio

It was defended on

June 6, 2024

and approved by

Thesis Advisor: Dr. Simon Barratt-Boyes, BVSc, PhD, DACVIM, Professor, Infectious Diseases and Microbiology, School of Public Health, University of Pittsburgh

Committee Member: Dr. Ernesto Marques, MD, PhD, Associate Professor, Infectious Diseases and Microbiology, School of Public Health, University of Pittsburgh

Committee Member: Dr. Laurie Silva, PhD, Assistant Professor, Pediatrics, School of Medicine, University of Pittsburgh

Exploring Ancestry-Related Differences in Dengue Virus Infection in Human Skin

Jocelyn Marie Taddonio, MS

University of Pittsburgh, 2024

Dengue is the most prevalent arboviral infection in the world, and the number of clinical cases and global spread are rising. Recent data have demonstrated a link between genetic ancestry and susceptibility to dengue virus (DENV) infection; individuals with European ancestry (EA) have a higher rate of infection and inflammatory response to dengue than those of African ancestry (AA). Immunofluorescence staining of skin – the site of dengue virus transmission – has illustrated differences in cytokine expression in EA and AA donors following infection *ex vivo*. Single nucleotide polymorphisms (SNPs) of various innate immune genes, including *RXRA*, have been associated with susceptibility to DENV infections and genetic ancestry. Retinoid X receptor alpha (RXRα) is known to promote proinflammatory responses by limiting interferon production and inducing inflammatory and chemokine gene expression. This inhibits host antiviral defenses, which makes the immune system more susceptible to viral infection. The possible role of RXRα in DENV infections is unknown, but it could influence the ancestry-related differences observed in immune responses to DENV infections. This study aims to examine RXRα expression in the epidermis, as well as identify the cells responsible for production of proinflammatory and antiviral cytokines during DENV infections. To investigate this, human skin explants donated by the University of Pittsburgh Medical Center (UPMC) were infected with DENV. Chemiluminescent western blotting and flow cytometry techniques were used to identify and quantify RXRα expression within infected cells. Full-thickness cell lysates (epidermal and dermal cells) suggested a difference in RXRα expression between ancestry donors 24-hours post infection, while

epidermal cell lysates showed no protein difference. Interleukin-1β (IL-1β) and interferon alpha (IFNα) concentrations were measured by ELISA to evaluate cytokine production in response to infection. Secreted cytokines were not detectable by ELISA 24-hours post infection, while preliminary data for intercellular cytokine levels showed no difference in concentration. This project was unable to identify the epidermal cells responsible for cytokine production in response to DENV infections. By understanding ancestry-related differences in DENV infections and the forces which drive the immune responses, therapeutics can be developed to modulate these responses that increase risk of disease in susceptible populations.

Table of Contents

List of Tables

List of Figures

Acknowledgements

Dr. Simon Barratt-Boyes – For trusting me with this project and helping to develop me into the scientist that I am today. I am extremely grateful for all of the opportunities that you have afforded me within this lab, both with the dengue project as well as the studies in the RBL.

Dr. Ernesto Marques and Dr. Laurie Silva – For the incredible insights, advice, and guidance that helped improve this project. Thank you for your mentorship.

Dr. Priscila Castanha – For often reminding me that "science will break your heart" when dealing with failed experiments or disappointing data, and always encouraging me that my western blots are prettier than I believe they are.

Michelle Martí – For allowing me to be your shadow in the lab. I have learned so much from you, not only about the dengue project, but how to become a more critical and forward-thinking scientist. Thank you for having an incredible amount of patience while training me, especially when I made mistakes and asked infinite questions, both in person and over text.

Morgan Ritchie – For all the Mario's trips, sushi dates, coffee runs, Instagram reels, and your wonderful friendship that sustained me throughout the past three years.

Meg Wallace and Hasitha Chavva – For being a joy to spend time with every day in lab, and always offering me a hug when I needed one.

The Three Rivers Battalion – For providing the flexibility and financial ability to pursue a master's degree while training to become an officer in the United States Army. This we'll defend!

My family – For the unwavering love and encouragement throughout my academic career to help me get to this point; I could not have done this without you.

1.0 Introduction

Dengue is the most prevalent mosquito-borne viral infection in the world, and it is endemic in over 100 countries within Central and South America, Africa, and Southeast Asia (1). Spread through mosquitoes, there are four circulating serotypes of dengue viruses (DENV) that can result in a range of illness and severity. Infections can either be asymptomatic, manifest into a mild febrile illness, or develop into a severe, and sometimes fatal, hemorrhagic disease (1, 2). More than half of the world's population live in areas of risk for DENV infections, and it is estimated that there are around 390 million infections annually with 96 million of those cases displaying any symptoms (3). Upon initial infection, individuals receive life-long immunity to the infection serotype, but only short-term immunity to the other three viral serotypes. After this immunity wanes, infection with another serotype will generate a secondary infection, which is more likely to develop into severe disease, a consequence of antibody-dependent enhancement (4). Dengue is continuing to spread to non-endemic regions of the world, such as the United States of America and Europe, and is considered as a major public health challenge by the World Health Organization.

1.1 Dengue Overview

1.1.1 Vector Global Distribution

As an arboviral infection, DENV is transmitted to humans through the bite of an infected female mosquito. Two mosquito species are responsible for the spread of this infection: *Aedes aegypti* and *Aedes albopictus* (5). Both mosquitoes are capable of transmitting other viruses of the *Orthoflavivius* family that DENV belongs to, such as Zika virus (ZIKV) and yellow fever virus (YFV) (6). *Ae. aegypti* primarily resides in tropical and subtropical regions, and inhabits areas such as the Caribbean, Central and South America, Africa, and southeast Asia (Figure 1). While *Ae. albopictus* are sympatric and partially share the same geographical range as *Ae. aegypti,* they additionally inhabit more temperate climates as well. Since the 1980s, *Ae. albopictus* have spread to the eastern United States and southern Europe (Figure 1).

Predicted Global Distribution of *Aedes aegypti*

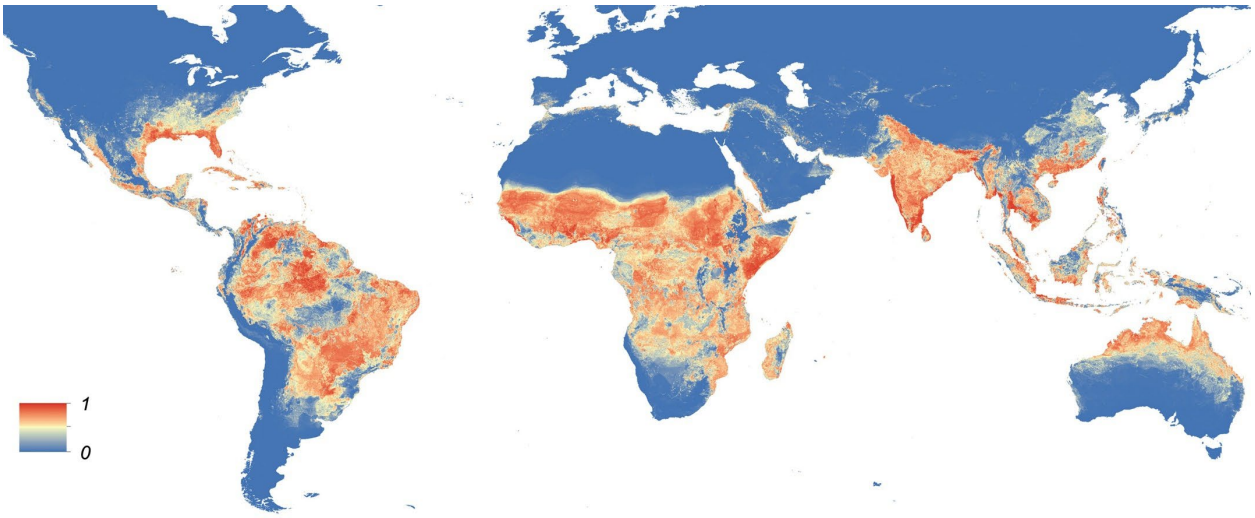

Predicted Global Distribution of *Aedes albopictus*

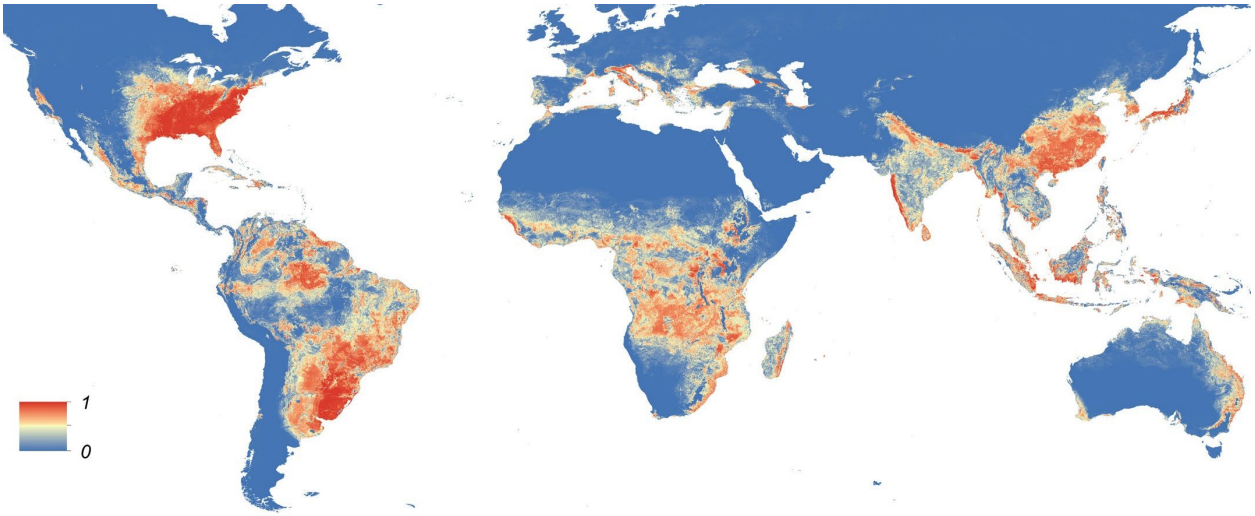

Figure 1. Geographical range of *Aedes aegypti* and *Aedes albopictus*

The predicted global range of two common arboviral vectors. The map depicts the probability of occurrence (from 0 blue to 1 red) at a spatial resolution of 5 km × 5 km. Figure obtained from eLife.08347 (Open Source).

Ae. aegypti are the primary vector for DENV, while *Ae. albopictus* can also transmit the virus, albeit less efficiently than the aforementioned (7). *Ae. aegypti* are anthropophilic and preferentially feed on humans, while *Ae. albopictus* are less attracted to humans and also feed from non-human mammalian hosts (7). Both mosquitoes predominantly feed during the day, when humans are most active. *Ae. aegypti* thrive in urban areas with high human population densities to feed from, and where they utilize artificial containers and open water reservoirs for breeding sites (5–7). With vaccine development still underway, disease prevention strategies focus primarily on vector control and managing mosquito breeding sites.

1.1.2 Global Burden of Dengue

Dengue has become the most widespread arbovirus in the world, with around 4 billion people living in areas with risk of infection (8). Over 100 countries in southeast Asia, the Americas, Africa, and western Pacific are endemic with dengue (1). The extensive range of dengue transmission is illustrated by reported cases of autochthonous or locally acquired dengue in tropical and subtropical regions of the world (Figure 2), areas where *Ae. aegypti* and *Ae. albopictus* vectors are known to inhabit (Figure 1). There is estimated to be around 390 million dengue infections annually, with 96 million of those cases showing clinical manifestations (3). With such a substantial impact on global health, dengue has significant economic consequences on direct and indirect costs of disease. In the Americas, annual costs of dengue illness is estimated around $2.1 billion (9), while in southeast Asia, annual costs are estimated around $950 million (10). Estimated annual global cost of dengue is around $8.9 billion US dollars (2).

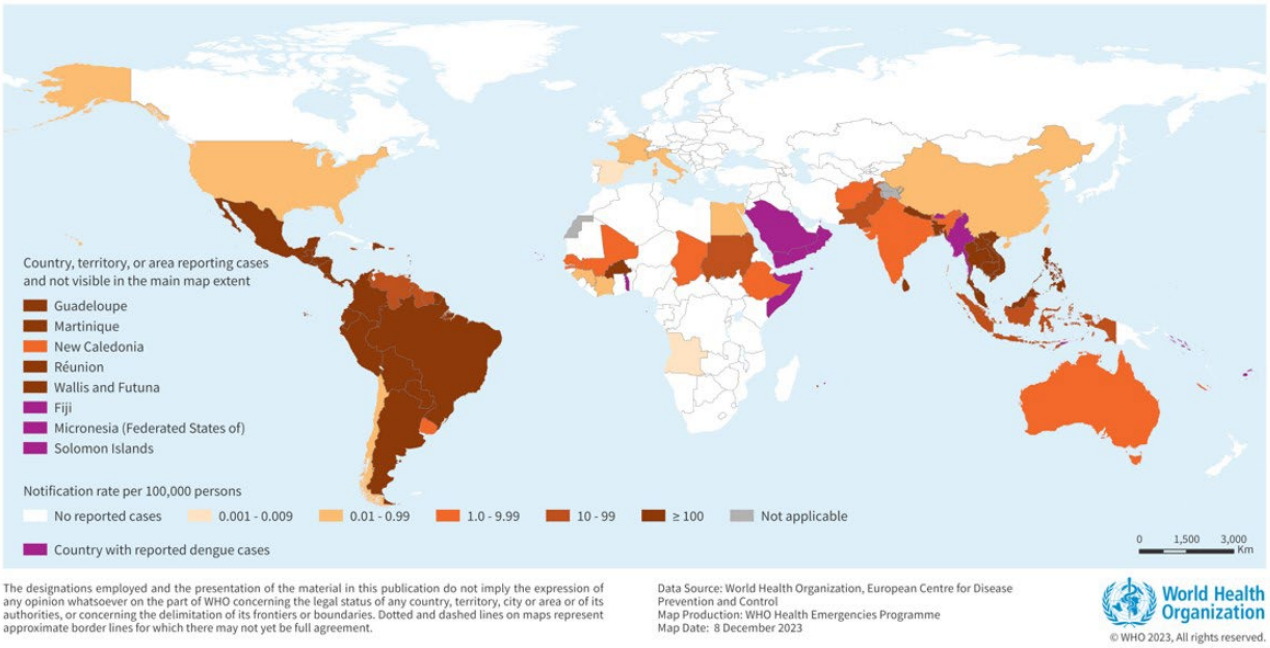

Figure 2. Global prevalence of dengue

Countries/territories/areas reporting autochthonous dengue cases (November 2022 - November 2023). Figure obtained from the World Health Organization (21 December 2023), Disease Outbreak News; Dengue – Global situation (Open Source).

The increasing spread of dengue is contributed to several factors, such as climate change, urbanization, and global travel (2). Changes in climate can expand the global range of vectors, as a rise in temperature can make previously uninhabitable areas more suitable for vectors. With the spread of mosquito vectors to new areas such as the United States of America and Europe (Figure 1), so too does the expansion of dengue infection increase (Figure 2). Urbanization enhances vector breeding by increasing breeding sites and human exposure to vectors. Global travel quickly introduces viruses from one area to another, contributing to the transmission of dengue as well (1). Due to its widespread prevalence worldwide, impacts on human health, and economic burden, dengue is a major global public health concern.

1.1.3 Disease Symptoms

Dengue has a wide spectrum of clinical manifestations, even though the majority of infections are asymptomatic (2). Infection can be caused by any of the four DENV serotypes, and following a bite from an infectious mosquito, symptoms typically develop within two weeks. After symptom onset, the illness goes through three phases: febrile, critical, and recovery (11, 12). The febrile phase typically lasts around 2-7 days, and includes symptoms of high fever, body aches, headaches, muscle and joint pains, nausea and vomiting, and development of a rash at the site of infection. After the fever clears, the critical phase begins and can last between 2-3 days (11, 12). The critical phase occurs in cases of severe dengue, which are more likely to develop from secondary infections. Patients with severe dengue display one or more of the following symptoms: plasma leakage which leads to shock, severe bleeding, or organ failure (12). During the recovery phase, the patient may experience tiredness and weakness as the infection clears.

1.1.4 Innate Immunity

Dengue infection begins when the virus is inoculated into the skin by a mosquito probing for a blood meal. Keratinocytes, the most abundant cell type in the epidermis, are among the first to become infected with the virus (13, 14). Once infected, these cells stimulate the immune response by producing proteins called cytokines and chemokines to recruit other immune cells to the site of infection. Skin resident immune cells including Langerhans cells, macrophages, and dermal dendritic cells, are recruited to the site of infection to aid in the immune response (13). As a result, these cells become infected with DENV as well, and contribute to the spread of infection to the dermis (13). Infected Langerhans cells and dermal dendritic cells eventually migrate to the

lymph nodes, where they initiate the adaptive immune response (14). Within the lymph nodes, virus can spread to other monocytes and macrophages, and DENV can continue to rapidly spread and disseminate throughout the body from this site through viremia.

1.2 Host Risk Factors

Infectious diseases rely on the dynamic relationship between pathogen, host, and environmental factors to cause disease. Host factors describe traits of individuals that have effects on disease susceptibility and severity, and they include characteristics such as age, genetics, comorbidities, and immune function (15). In severe dengue, mortality rates can be greatly decreased if cases are promptly recognized and supportive care is provided. Age, history of diabetes, pregnancy, and secondary infections were found to be risk factors for development of severe dengue rather than dengue fever (16). Understanding host factors for a disease can provide knowledge about viral transmission and host-pathogen interactions, which is crucial for designing and improving therapeutic treatments.

1.2.1 Genetic Variations

Genetic variations are the differences that vary in DNA from one person to the next, and they can have an expansive effect on the human body and its many biological functions. These variations are most commonly caused by mutations, specifically single nucleotide polymorphisms (SNPs) that occur in a single base pair in a given DNA sequence (17). SNPs are very prevalent in the genome, occurring on average once every 1,000 nucleotide bases, which can result in millions

of SNPs within a single genome (18). Some variations do not change amino acid sequences for protein synthesis and are known as silent mutations, while others can cause changes within a protein sequence (termed non-synonymous) that have no detectable effect on protein function (17, 19). However, some mutations (termed synonymous) can alter the functionality of the genes they reside in, the structure of proteins they produce, and various biological processes they are involved in. As such, SNPs can play a role in infectious diseases by affecting susceptibility to infections, disease severity and progression, as well as the body's immune response to a certain pathogen (20).

There are often patterns of frequencies in SNPs between geographical populations and ethnicities. Ancestry-informative markers (AIMs) are sets of SNPs distributed throughout the genome that appear more frequently in certain geographical regions of the world, and they are used to estimate the proportion of genetic ancestry of individuals (21, 22). These AIMs occur in high frequencies across continental populations, such as Africa, Asia, and Europe, and can distinguish proportion of ancestry from these populations through a Principal Component Analysis (PCA) (22, 23). Our lab uses these AIMs to distinguish proportion of genetic ancestry of tissue donors since self-identification is not the most accurate representation of genetic background.

1.2.2 Ancestry and Severe Dengue

Epidemiological studies from several Central and South American countries, such as Cuba and Colombia, as well as Africa have identified ancestry as a potential risk factor for the development of severe dengue (24–27). These studies observed that individuals with European ancestry (EA) are more susceptible to severe dengue than those of African ancestry (AA). During an outbreak in Cuba, significantly higher amounts of dengue cases were reported in Cubans of

European ancestry compared to those with African ancestry (24). This confers some protection against viral infection in those with African ancestry, as they are less susceptible to disease.

1.2.3 SNPs Associated with Dengue Severity and Ancestry

Genome-wide association studies (GWAS) are a common tool to study associations between SNPs and phenotypic traits, such as disease symptoms and illness. To do this, GWAS research can identify which variations occur in higher frequencies within cases of diseases than compared to a healthy population (28). Cuba has a unique advantage of studying the implicated relationship between genetic ancestry and dengue susceptibility as it has frequent, but isolated, dengue epidemics and is composed of a diverse population of admixed-ancestry. Using GWAS, a Cuban cohort of patients with dengue fever was analyzed for SNPs and matched with asymptomatic controls (25). This study identified functional SNPs within innate immune genes associated with ancestry and susceptibility to dengue infections, with two genes of note including oxysterol binding protein-like 10 (OSBPL-10) and retinoid X receptor alpha (RXRα) (25). This study suggests that RXRα plays a role in African ancestry protection against dengue fever.

1.3 Retinoid X Receptor Alpha (RXRα)

Retinoid X receptors (RXRs) are a family of nuclear receptors within cells that contribute to various biological processes, including cell differentiation, metabolism, and immune responses. RXRs can either homodimerize with themself or become heterodimers with other nuclear receptors like peroxisome proliferator-activated receptor (PPAR), retinoic acid receptor (RAR), and vitamin

D receptor (VDR) (29–31). Different RXR homo- and heterodimers recognize and bind to distinct promoter sites, which affects which biological pathway they influence. With numerous combinations of ligands that RXRs can heterodimerize with, these receptors can function in many signaling pathways (29). RXRs are made up of three subtypes: RXRα (NR2B1), RXRβ (NR2B2), and RXRγ (NR2B3) (29, 32).

1.3.1 Cellular Localization and Receptor Function

In the nucleus, RXRα serves as a ligand activated transcription factor to regulate gene expression involved in various biological processes. Natural ligands of RXRα include 9-*cis*-retinoic acid, docosahexaenoic acid (DHA), and phytanic acid, and several other synthetic ligands called rexinoids that can also bind to RXRα (29, 33). Additionally, various cellular processes can cause RXRα to migrate from the nucleus to the cytoplasm, including differentiation, apoptosis, and inflammation (30, 31). Nongenomic functions of RXRα typically involve a cleaved or modified form of the protein (31). One function of cytoplasmic RXRα includes exporting nuclear receptor TR3 from the nucleus to the cytoplasm, where it can promote apoptosis (34). RXRα has also been implicated to be regulators of inflammatory pathways in T cells, macrophages, and dendritic cells, and shown to suppress the growth and spread of cancer cells (30, 35). However, the cytoplasmic functions of RXRα are not as well studied as its nuclear functions.

1.3.2 Role in Viral Infections

RXRα is abundantly expressed in the epidermis and other mammalian organs, such as the kidneys, intestines, and liver, and so, it has a lot of possible roles in skin (29, 32). RXR-LXR

participates in AP1 signaling in keratinocytes and has demonstrated effects on epidermal keratinocyte proliferation and differentiation in mice (36–38). Ablation of this receptor in keratinocytes results in abnormalities in cell proliferation and differentiation, and an induced inflammatory reaction (38, 39). It also has been shown to regulate metabolism and immune functions of macrophages, with a reduced expression of RXRs during HIV infections in these cells (40, 41). Retinoids and rexinoids have been used in various clinical settings to treat various skin conditions, such as acne, psoriasis, and some cancers. Isotretinoin is a drug administered for acne treatment, and studies have shown that there is an association between the use of this retinoid and HSV-1 infections, suggesting that the receptor has an impact on viral susceptibility and immunity (42).

Studies are beginning to unravel the role of RXRα within viral infections. RXRα has been implicated in modulating inflammation and immune responses by regulating cytokine and chemokine expression during innate immune responses (37, 42). Within VSV infections, it has been shown to inhibit type I interferon production which increases host cell susceptibility and risk of infection (Figure 3). To summarize Figure 3, ligand activation of RXRα indirectly inhibits interferon production through a β-catenin pathway, which ultimately reduces antiviral gene expression. As RXRα expression is downregulated in viral infections, this promotes the production of interferons which contribute to the host's antiviral response (Figure 3). RXRα also promotes proinflammatory responses by inducing chemokine gene expression in myeloid cells and recruiting cells to the site of inflammation (37). The role of RXRα in dengue viral infections is unknown. The focus of this study will be to examine RXRα within the epidermis during early dengue viral infections.

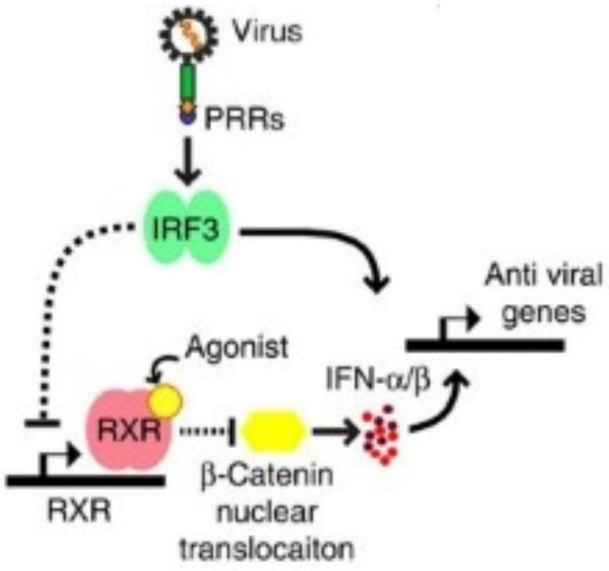

Figure 3. RXRα inhibits type I interferon production

Working model for RXRα regulating host antiviral responses. Dash line: indirect regulation. In viral infections, RXRα expression is downregulated, which promotes interferon production to activate expression of antiviral genes. Figure taken with permission from Ma, F., et al, Retinoid X receptor a attenuates host antiviral response by suppressing type I interferon, https://doi.org/10.1038/ncomms6494.

1.4 Experimental Results

By using an *ex vivo* human skin model, early immune and cellular responses to DENV infections can be investigated. Our lab utilizes this model to observe the early biology of dengue infections through mimicking mosquito probing and inoculation by stabbing virus into the tissue with a bifurcated needle. Through the quantification of immunofluorescent staining, differences in rates of infection, migration of macrophages to the site of infection, and infected migrated macrophages within infected EA and AA tissue are observed. These data show higher rates of infection in EA donors compared to AA donors within both the epidermis and dermis.

Additionally, EA donors have higher rates of macrophage recruitment and infection of macrophages than AA donors. The production of cytokines at various time points post-infection details the type of immune response that is induced. Individuals of EA produce significantly more interleukin-1β (IL-1β), which corresponds to a more proinflammatory response in the skin. Alternatively, there are higher levels of interferon α (IFN-α) production in those of AA, which aligns more with an antiviral response. The source of these immune differences is unknown.

An analysis of SNPs has been conducted in our lab to determine if there was a correlation between dengue infection and ancestry with the presence of these SNPs. Previous donor samples with corresponding data on infection rates and genetic ancestry analysis were genotyped for these SNPs. The results demonstrate that SNPs in genes such as *RXRA*, OAS1, 2, and 3 are significantly correlated with genetic ancestry and dengue infections. This suggests that the ancestry-related differences observed in dengue infections may have some connection with the presence of these SNPs. Investigation into these proteins could provide insight into the ancestry-related differences in response to dengue infections.

2.0 Specific Aims

Studies have demonstrated a relationship between genetic ancestry and susceptibility to dengue infections, which shows that individuals with European ancestry (EA) have higher rates of infection and a more proinflammatory response to dengue than those of African ancestry (AA). The source of these immune differences is unknown. SNPs in innate immune genes associated with dengue susceptibility and genetic ancestry have been identified (25). *RXRA* was one of the genes implicated (25), and it is highly expressed in the epidermis (29). In viral infections, RXRα has been shown to inhibit interferon production to attenuate host anti-viral responses and promote proinflammatory responses (37, 42). The role of RXRα in dengue infections is unknown. These SNPs in RXRα may have a potential role in influencing the ancestry-related differences in immune responses to dengue viral infections. The purpose of this study is to examine RXRα expression in human skin, as well as to investigate cytokine production in response to dengue viral infections.

2.1 Aim 1: Investigate RXRα Expression in Human Skin Following DENV Infection *ex vivo* and *in vitro*

Hypothesis: In response to dengue virus infection, expression of RXRα will be high in tissue of European ancestry and low in tissue of African ancestry.

Experimental Approach: Chemiluminescent western blotting will be used to detect RXRα protein within full-thickness and epidermal cell lysates of EA and AA. Samples will include a 0-hour baseline control, a 24-hour mock infection timepoint, and a 24-hour post DENV infection

timepoint. Quantification of western blots using ImageJ software will normalize bands with housekeeping protein, glyceraldehyde-3-phosphate dehydrogenase (GAPDH), and will provide relative protein abundance to compare RXRα expression across samples. Complementary staining of infected epidermal cells will quantify protein levels of RXRα by flow cytometry.

2.2 Aim 2: Determine the Epidermal Cells Responsible for Cytokine Production in Response to DENV Infections *in vitro*

Hypothesis: Keratinocytes will be the primary cell responsible for producing IL-1β in the epidermis following DENV infection.

Experimental Approach: Staining of epidermal cells following *in vitro* DENV infection will be analyzed through flow cytometry to characterize cell populations and rates of infection within the epidermis. Samples will include a 24-hour mock infection timepoint and a 24-hour post DENV infection timepoint with donors of both EA and AA. Secreted and intracellular cytokine concentrations for IL-1β and IFNα will be measured using an enzyme-linked immunosorbent assay (ELISA) within EA mock and DENV infected samples.

3.0 Materials and Methods

3.1 Skin Donors

Human skin explants were donated by the University of Pittsburgh Medical Center (UPMC) from discarded tissues following elective pannilectomies and abdominoplasties. All donors are anonymized, and ancestry is based on patient self-identification. This is confirmed through genetic analysis with a panel of 128 ancestry informative markers to determine the proportion of biogeographical ancestry within each donor. Skin donor (SD) nomenclature is as follows: identification number/ year of collection/ ancestry (European ancestry – EA, African ancestry – AA).

3.2 Skin Processing

Subcutaneous fat was trimmed off the tissue using sterile forceps and scissors, taking along with it a thin layer of the dermis. The remaining tissue was rinsed with 1X PBS and cut into smaller strips. Following trimming, the skin can either be processed the same or the next day, depending on the time that the tissue was received. If processing the following day, the tissue was left floating on skin media (Table 2) overnight with the epidermal layer facing up and dry. To begin processing, the tissue was pinned down by needles, with the epidermal surface dry and facing upward. A Goulian skin graft knife (Medline) with a fresh razor blade was used to remove slices of split-thickness skin. These sections were cut into squares and incubated at 37°C in 1.0 mL of 1:10

dispase (Sigma Aldrich) in PBS in a 24-well plate for 1 hour. After incubation, the epidermal layers were separated from the dermal layers using two sterile forceps.

3.3 Epidermal Cell Suspensions

10.0 mL of trypsin was placed in a 37°C water bath while layers of the skin were separated during skin processing. Once all the epidermal sheets were collected, they were added to the pre-warmed 10.0 mL of trypsin and incubated in the 37°C water bath for 6 minutes. Following incubation, the epidermal sheets were homogenized in trypsin 25-50 times with a serological pipette. 10.0 mL of skin media was added to neutralize the trypsin, and the suspension was filtered through a 100 μM cell strainer (Corning) and centrifuged at 500 g for 10 minutes at 4°C. The supernatant was decanted, and the cell pellet was resuspended in 20.0 mL of skin media. Epidermal cells were counted and aliquoted based on future experiments.

3.4 DENV Infection

Fresh epidermal cell suspensions were infected with DENV-2 (strain 16681) at a multiplicity of infection (MOI) of 2 for 24 hours. Mock experimental samples were resuspended in skin media in place of virus. Once virus was added, mock and infected suspensions were incubated at 37°C for 2 hours in 15 mL conical tubes, mixing every 30 minutes to prevent cells from settling at the bottom. After 2 hours, the total volume of each suspension was transferred to separate wells on a 24-well, low-binding affinity plate (Corning) and topped with skin media. The

plate was incubated for 22 hours at 37°C. At the 24-hour timepoint, the suspensions were collected from the plate and centrifuged at 500 g for 5 minutes at 4°C. The supernatant was collected and frozen at -80°C for ELISAs, and cells were collected for flow cytometry or lysates.

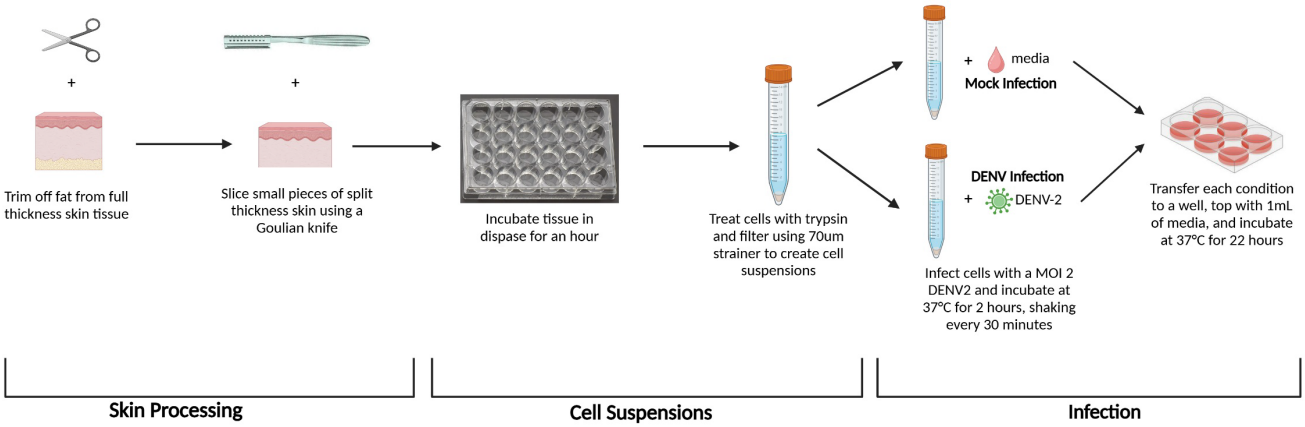

Figure 4. Schematic of tissue processing, cell suspension, and infection protocol

Image created with BioRender.com.

3.5 Cell Lysates

Cells were collected and centrifuged into a pellet at 500 g for 5 minutes at 4°C. The resulting supernatant was removed, and the cells were resuspended in 200.0 µL of RIPA buffer (Table 2) and 2.0 µL of protease inhibitor (ThermoScientific). The solution was incubated on ice for 2 hours, with a brief vortex every 30 minutes. After complete incubation, the cells were vortexed four times for 10 seconds, incubating on ice in between each vortex. Lysed cells were centrifuged at 24,000 g for 15 minutes at 4°C, and the supernatant was collected and frozen down for later use.

3.6 Western Blots

Lysates were diluted in a solution of RIPA buffer and protease inhibitor at a 1:4 dilution. 25 µL of prediluted BCA standards (Cat #23208, ThermoScientific) and lysates were added to a 96-well plate (Costar), after which 200 µL of 50:1 BCA Reagent A (Cat #23228, ThermoScientific) and BSA Reagent B (Cat #23224, ThermoScientific) was pipetted into each well. Plates were rocked for 30 seconds and incubated at 37°C for 30 minutes. Optical density was determined at the wavelength 562 nm by using a SpectraMax Plus 384 microplate spectrophotometer with the SoftMax Pro software version 6.4 (Molecular Devices). Protein concentrations were calculated using a simple linear regression analysis in GraphPad Prism 10.2.2.

Preparation of samples were created with cell lysates, Novex 4X Bolt LDS sample buffer (Cat #B0007, ThermoFisher), Novex 10X Bolt sample reducing agent (Cat #B0009, ThermoFisher), and PBS. Samples were spun and heated at 70°C for 10 minutes. While heating, a Bolt 4-12% Bis-Tris Plus 15 well gel was placed into an Invitrogen Bolt mini gel tank (ThermoFisher), and the gel chamber was filled with MES Running buffer (Table 2). Wells in the gel were rinsed with running buffer before loading with 25 µL of samples and 10 µL of Novex SeeBlue Plus2 Prestained Protein Standard (ThermoFisher) per well. Gels were run for 20 minutes at 200V using a PowerPac Universal power supply. After the proteins migrated down the gel, they were transferred to a nitrocellulose membrane by running for 2 hours at 10V in a Bolt transfer module within the gel tank filled with transfer buffer (Table 2). Once the transfer was complete, the membrane was blocked with 5.0% milk in 0.05% TBS-T (Table 2) for 1 hour, rocking. Following blocking, the membrane was incubated with GAPDH (Proteintech) and RXRα (Proteintech) primary antibodies at a 1:10,000 dilution in 5.0% milk in TBS-T overnight while

rocking at 4°C. The next day, the membrane was rinsed 3 times for 5 minutes each with 0.05% TBS-T before incubating with secondary antibodies for 1 hour, rocking. Secondary antibodies included a goat anti-mouse IgG antibody (ThermoFisher)at a 1:200,000 dilution in 0.05% TBS-T and a goat anti-rabbit IgG antibody (ThermoFisher) at a 1:100,000 dilution in 0.05% TBS-T to detect GAPDH and RXRα primary antibodies, respectively. After incubation, the membrane was rinsed 3 times for 5 minutes each with 0.05% TBS-T before being placed in 500 µL of both SuperSignal West Pico Plus Stable Peroxide and Luminol/Enhancer (ThermoScientific) for a 5-minute incubation.

Once the membrane has been exposed to chemiluminescent substrates, it was developed using an Amersham 600 Imager. Images were analyzed in ImageJ software to obtain pixel density of protein bands and their respective background. Using Excel, the pixel density of bands and background (X) were inverted using the formula 255 - X. With inverted values, the net value of each band was calculated by subtracting the inverted background from the inverted band value (i.e. net value = band – background). Relative quantification of RXRα was calculated by taking the ratio of the protein of interest by the loading control (net value of RXRα/net value of GAPDH).

3.7 Flow Cytometry Staining

Cells were added to a 96-well, v-bottom plate (Costar) and centrifuged twice with 200 µL of MACs buffer (Table 2) at 2,000 rpm for 5 minutes at 4°C. 100 µL of diluted Live/Dead viability stain (Table 1) and 5 µL of Fc block (BD Biosciences) was added per well and incubated in the dark at 4°C for 15 minutes. Cells were washed twice again with MACs buffer, and then fixed and permeabilized by incubating in 100 µL of BD Cytofix/Cytoperm (BD Biosciences) for 20 minutes

in the dark at room temperature. After incubation, the cells were washed with BD Perm/Wash (P/W) (BD Biosciences) twice and resuspended in primary DENV antibody (Table 1) overnight in the dark at 4°C for around 16-18 hours.

The following morning, the cells were washed 3 times in P/W and once in MACs buffer. Cells were resuspended in 200 µL of MACs buffer and incubated at 4°C until ready to stain later in the day; this was to prevent cells from incubating in secondary antibody for over 24 hours. To resume staining, the plate was centrifuged at 2,000 rpm for 5 minutes at 4°C. Cells were resuspended in 200 µL of P/W and incubated at room temperature for 15 minutes. Once the cells had re-permeabilized, the plate was centrifuged at 2,000 rpm for 5 minutes at 4°C and resuspended in goat anti-mouse IgG2a secondary antibody, CD45, HLADR, CD1a, RXRα, and AE1/AE3 antibodies (Table 1) overnight in the dark at 4°C for around 16-18 hours. The next morning, the cells were washed 3 times in P/W and twice in MACs buffer. Following the last centrifugation, cells were resuspended in 200 µL of MACs buffer in FACs tubes (Corning) and stored at 4°C until ready to analyze. Samples were acquired on a BD FACSymphony A5 SE cytometer using BD FACSDiva Software and analyzed on FlowJo 10.10.0.

Table 1. Antibodies Used in Staining for Flow Cytometry

Fluorophore	Antigen	Conc./Dilution	Catalog #	Manufacturer
Yellow	LIVE/DEAD fixable yellow dead cell stain	1:200	L34968	ThermoFisher Scientific
R718	CD45	0.0002 µg/well	566962	BD Biosciences
AF488	AE1/AE3	0.5 µg/well	53-9003-82	ThermoFisher Scientific
RB780	HLADR	0.0002 µg/well	755886	BD Biosciences
BV421	CD1a	0.00005 µgwell	563939	BD Biosciences
N/A	anti-dengue virus complex	0.01 µg/well	MAB8705	Millipore Sigma
PE	Gt α-Ms IgG2a	0.15 µg/well	31863	ThermoFisher Scientific
AF594	RXRα	0.0002 µg/well	sc-515929	Santa Cruz Biotechnology

3.8 ELISAs

Human IL-1beta/IL-1F2 (Cat# DY201) and Human IFN-alpha 2/IFNA2 (Cat# DY9345-05) DuoSet ELISA kits from R&D Systems were utilized. High-binding, half-area, 96-well plates (Corning) were coated with 50 µL of the working concentration of capture antibody in PBS and incubated overnight at room temperature. The following day, the plates were washed 3 times using a washing buffer consisting of 0.05% Tween 20 in PBS and were subsequently blocked with 150 µL of reagent diluent (1% BSA in PBS). After incubation at room temperature for 1 hour, the plates were washed and 50 µL of standards and undiluted samples were pipetted in duplicates. 50 µL of reagent diluent was added as a negative control. The plates were then incubated for 2 hours. Following additional washes, 100 µL of the working concentration of detection antibody was added to each well and incubated at room temperature for another 2 hours. Once the incubation was completed, the plates were washed and 100 µL of the working dilution of streptavidin-HRP

was added per well. The plates were incubated for 20 minutes at room temperature and were subsequently washed for a final time. 100 µL of TMB substrate (KPL SureBlue) was added to each well before incubating the plate for 20 minutes at room temperature. After the final incubation, 50 µL of 1N hydrochloric acid (HCl, Sigma) was pipetted per well. Optical densities were determined at the wavelengths 450 and 570 nm by using a SpectraMax Plus 384 microplate spectrophotometer with the SoftMax Pro software version 6.4 (Molecular Devices). Protein concentrations were interpolated from the standard curve generated with a four-parameter logistic (4-PL) non-linear regression curve in GraphPad 10.2.3.

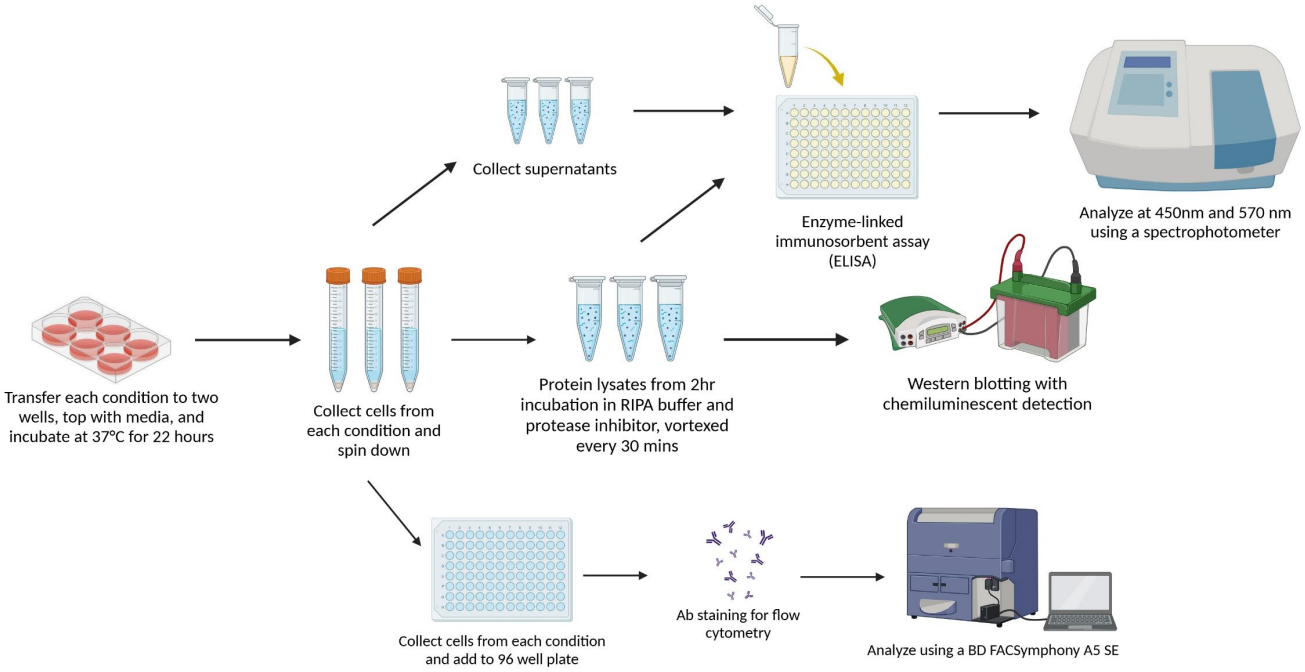

Figure 5. Schematic of experiments conducted with infected cells

Image created with BioRender.com.

Table 2. Buffer and Media Recipes

Buffer	Recipe
Skin media	RPMI (Invitrogen), 10% FBS (Atlanta Biological), 1% penicillin/streptomycin (Invitrogen), 1% L-glutamine (Invitrogen), 10mM HEPES (Invitrogen), 1% non-essential amino acids (Invitrogen), and 1% sodium pyruvate (Invitrogen)
RIPA buffer	10 mM Tris-Cl (pH 8.0), 1 mM EDTA, 1% Triton X-100, 0.1% sodium deoxycholate, 140 mM NaCl
MES Running buffer	50 mL 20X Bolt MES SDS (ThermoFisher), 950 mL MilliQ water
Transfer buffer	50 mL 20X Transfer buffer (ThermoFisher), 100 mL MeOH, 850 mL MilliQ water
0.05% TST-T	500 µL of Tween20 (Fisher BioReagents), 50 mL of 20X TBS (ThermoScientific), 949.5 mL MilliQ water
MACs buffer	420 mL 1X PBS, 5 mL 1M HEPES, 25 mL 0.1M EDTA, 50 mL 5% BSA in 1X PBS, and 150 µL 5M NaOH

4.0 Results

4.1 Aim 1: Investigate RXRα Expression in Human Skin Following DENV Infection *ex vivo* and *in vitro*

To reiterate, expression of RXRα is expected to be high in European ancestry (EA) donors, as it would inhibit interferon production and the antiviral immune response (42). This would additionally promote inflammation through increased chemokine expression, and increase susceptibility to disease (37). Alternatively, low expression of RXRα is predicted in donors of AA, allowing an unrestricted antiviral response through interferon production, which would explain the reduced susceptibility of infection within these individuals (Figure 6).

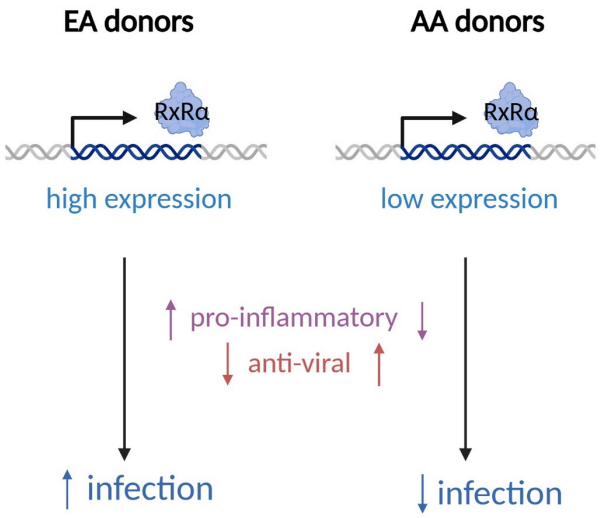

Figure 6. Schematic of Aim 1 hypothesis

Image created with BioRender.com.

4.1.1 RXRα Expression is Higher in European Ancestry than African Ancestry in Full-Thickness Cell Lysates

Using lysates created from full-thickness tissue, RXRα was detected at 51kDa in both EA and AA samples. The blot was stripped to remove previous antibodies and stained again for β-actin, which was detected at 42kDa. In the western blot, there appears to be consistently high expression of RXRα across 0-hour and 24-hour mock and infected samples in the EA donor. Alternatively in AA samples, there appears to be high expression of RXRα at 0-hr, but protein levels decreased following mock and DENV infection (Figure 7A). For a more quantitative analysis, the blot was analyzed using ImageJ to determine the relative protein expression of RXRα within each condition. Relative protein expression is conveyed as a ratio of RXRα to β-actin within the same lane. In the EA donor, there were relatively high levels of RXRα that slightly decreased between each timepoint. However, in the AA donor, there was relatively less RXRα in each timepoint compared to its EA counterpart. In AA tissue, RXRα was expressed the highest at 0-hours, but decreased after 24-hours mock infection and even more 24-hours post-DENV infection (Figure 7B). This data suggests that RXRα expression was unaffected by dengue infection in tissue of EA, whereas there was a drop of RXRα in donors of AA in response to DENV infection.

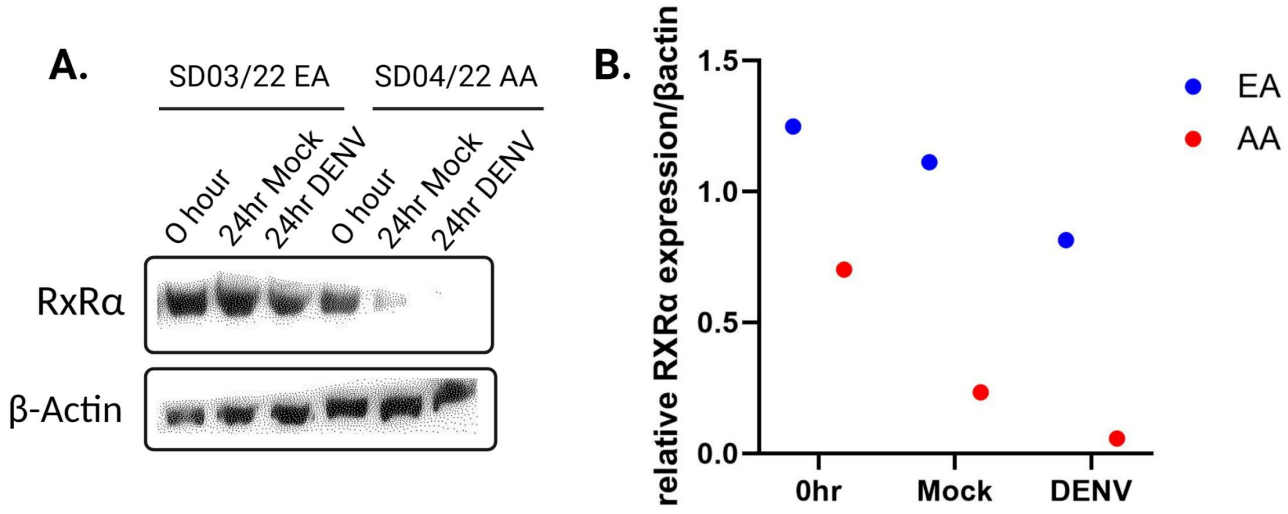

Figure 7. Detection and quantification of RXRα in full-thickness cell lysates

RXRα and β-actin detected in a western blot developed by Michelle Martí (A) and relative RXRα protein expression (B) at 0-hr, 24-hr mock, and 24-hr DENV infected timepoints in lysates of European and African ancestry.

4.1.2 Optimization of Western Blot Protocol

Since β-actin and RXRα were close in molecular weights (42kDa and 51kDa, respectively), they could not be detected simultaneously on the same blot. This required staining and detecting one protein before removing those antibodies with a stripping buffer, then re-staining the same blot with antibodies for the other protein. By stripping the membrane, there is a chance that some protein will be lost in the process, which can alter the detection of consecutive staining on the same membrane. To optimize this process, a housekeeping protein of a lower molecular weight was identified and stained in tandem with RXRα for simultaneous detection. All subsequent western blots used GAPDH for the loading control.

To improve the image quality of western blots, a change was made to the imaging process. The previous western (Figure 7A) was obtained using a film developer, a machine that frequently

required maintenance. Membranes were exposed to film and imaged using the developer in a dark room. As an alternative detection option, an Amersham 600 Imager was used to digitally detect proteins on a membrane. This proved to be a more efficient and effective method as it was a more sensitive machine that was easy-to-use, provided high resolution images, and had quantitative analysis capabilities. As a result, it was used for all prospective western blots.

BCA protein assays were used to measure protein concentrations within samples before they were added to a polyacrylamide gel for electrophoresis to ensure the same amount of protein was loaded into every well. Despite this assay, the expression of the GAPDH loading control varied between lanes (Figure 8A). This was a problem, as the loading control for westerns are supposed to be consistently equal across wells to not only confirm equal loading and transferring of samples, but to also compare signals of the protein of interest across wells. As a solution, densitometry analysis was used to normalize GAPDH expression within a western blot. For this, a membrane of samples would be stained for just GAPDH and following imaging, would be analyzed using ImageJ. The densitometry of each band was measured and normalized to a well with good protein expression. A new western blot was loaded with the same samples but using the normalized values instead, and this time were stained for both RXRα and GAPDH. The images from the normalized westerns show more equal expression of the loading control between each well (Figure 8B). This adjustment improved the quality of future western blots.

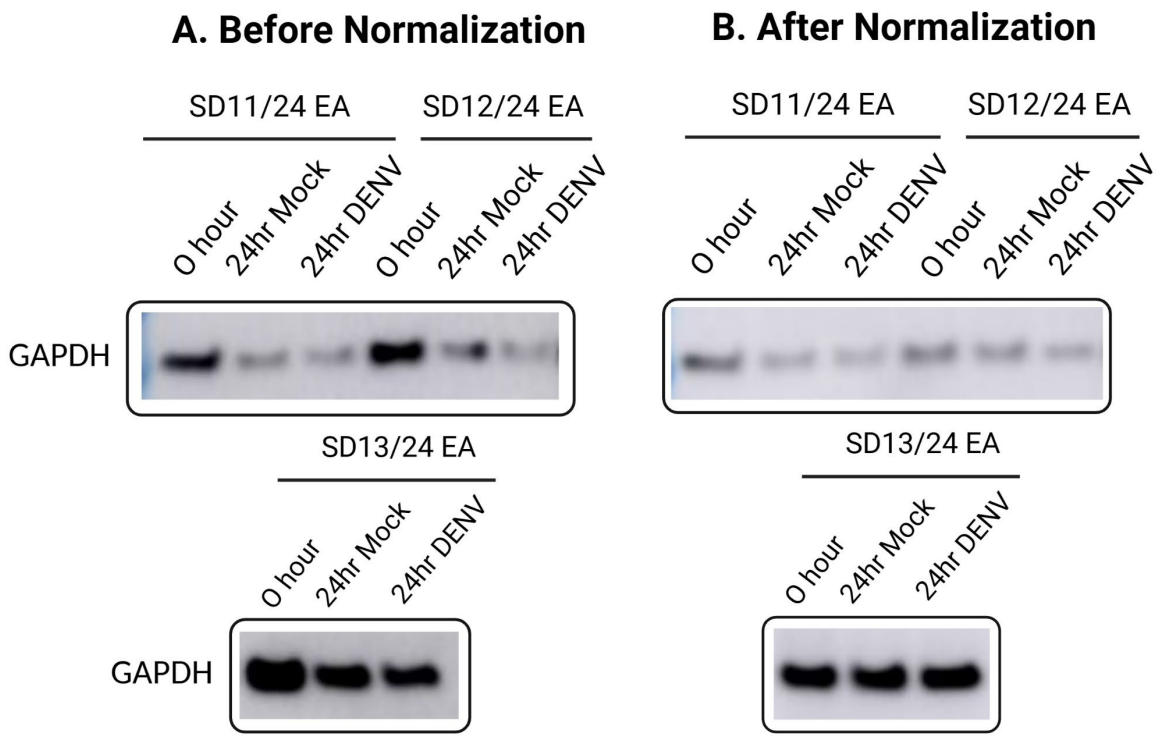

Figure 8. Normalization of GAPDH expression in western blots

Western blots before (A) and after (B) densitometry analysis to normalize the loading control, GAPDH, across samples.

4.1.3 RXRα is Detected and Quantified within Epidermal Cell Lysates

The full-thickness tissue in the previous western showed RXRα expression in lysates with epidermal and dermal cells combined (Figure 7). To get a better understanding of RXRα solely within the epidermis, lysates were made from epidermal cells that were infected in suspension. RXRα was simultaneously detected at 51kDa with GAPDH at 36kDa in lysates of both EA and AA (Figure 9). Based on the western blot images, the expression of RXRα varied. In SD11 and SD12, both donors of EA, RXRα expression appears to remain constant across all timepoints. However, another EA donor, SD13 appears to show lower RXRα expression in response to DENV

infection. Meanwhile, RXRα expression in AA donors appear to decrease in response to DENV infection (Figure 9).

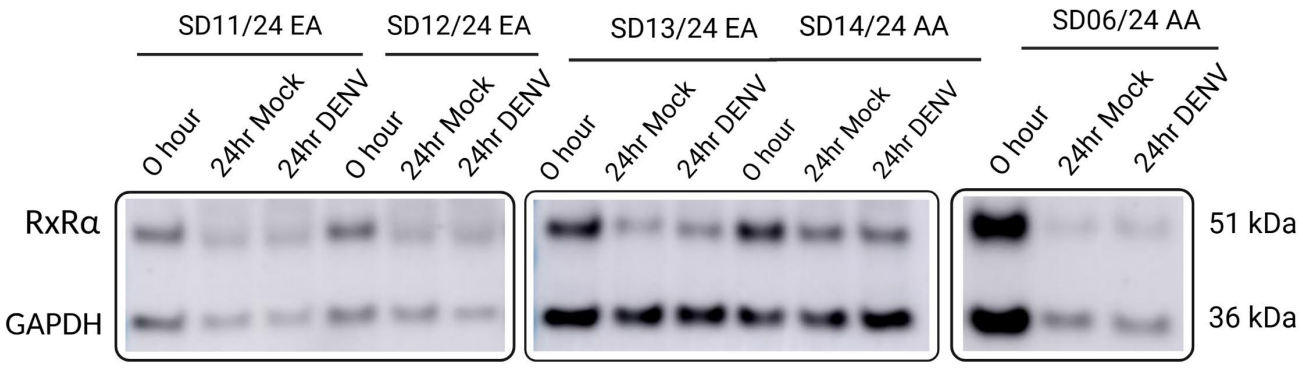

Figure 9. Detection of RXRα in epidermal cell lysates

RXRα and GAPDH detected in 0-hour, 24-hour mock, and 24-hr DENV infected timepoints in epidermal cell lysates of European and African ancestry.

Densitometry analysis was required for quantitative comparison among timepoints and donors in Figure 9, as well as to receive a better understanding of the change of RXRα expression in each sample. The relative protein expression of RXRα showed that unlike the results found in Figure 7, EA and AA donors showed similar expression of RXRα across timepoints (Figure 10). There is a decrease in RXRα after 24 hours, but there is no difference between mock and infected samples (Figure 10).

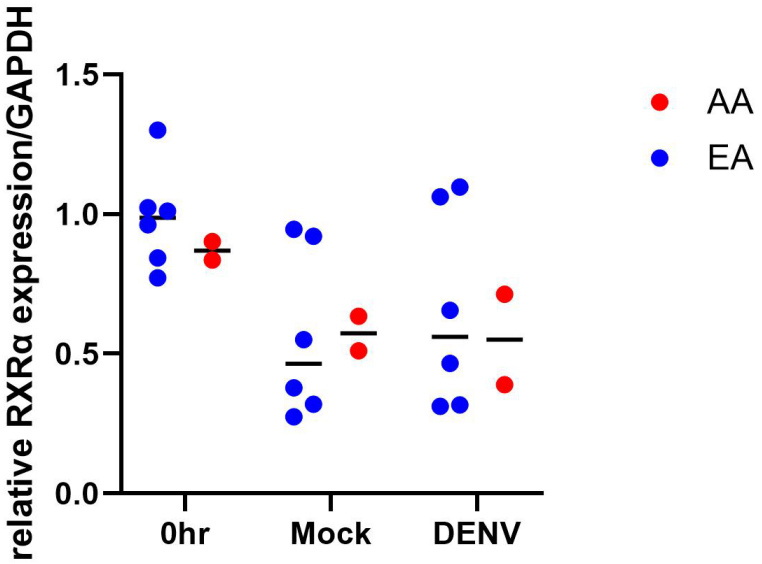

Figure 10. Quantification of RXRα in epidermal cell lysates

RXRα relative protein expression at 0-hour, 24-hour mock, and 24-hour DENV infected timepoints in lysates of European and African ancestry. Relative protein expression is a ratio of RXRα/GAPDH pixel density. Each dot represents a different donor.

4.1.4 Using Flow Cytometry to Detect RXRα in Epidermal Cells

Given the difficulties with the previous western blots, flow cytometry was used as an additional method to detect RXRα within epidermal cells. A RXRα antibody was added to a preexisting, functional antibody panel that included a stain for dead cells, epidermal cell markers, and an anti-dengue viral complex antibody. Mock and DENV infected cells were stained with this panel, and this experiment included a control that contained no antibodies (unstained) and a control stained with every antibody except RXRα (RXRα-). Analysis of mock and DENV+ cells showed small, distinct populations of RXRα (Figure 11). However, it is important to examine the control samples to ensure these are true populations. While the unstained control did not show any RXRα

population, there was an artifact in the RXRα- control (Figure 11). Therefore, this demonstrates the RXRα population in the mock and infected samples was false.

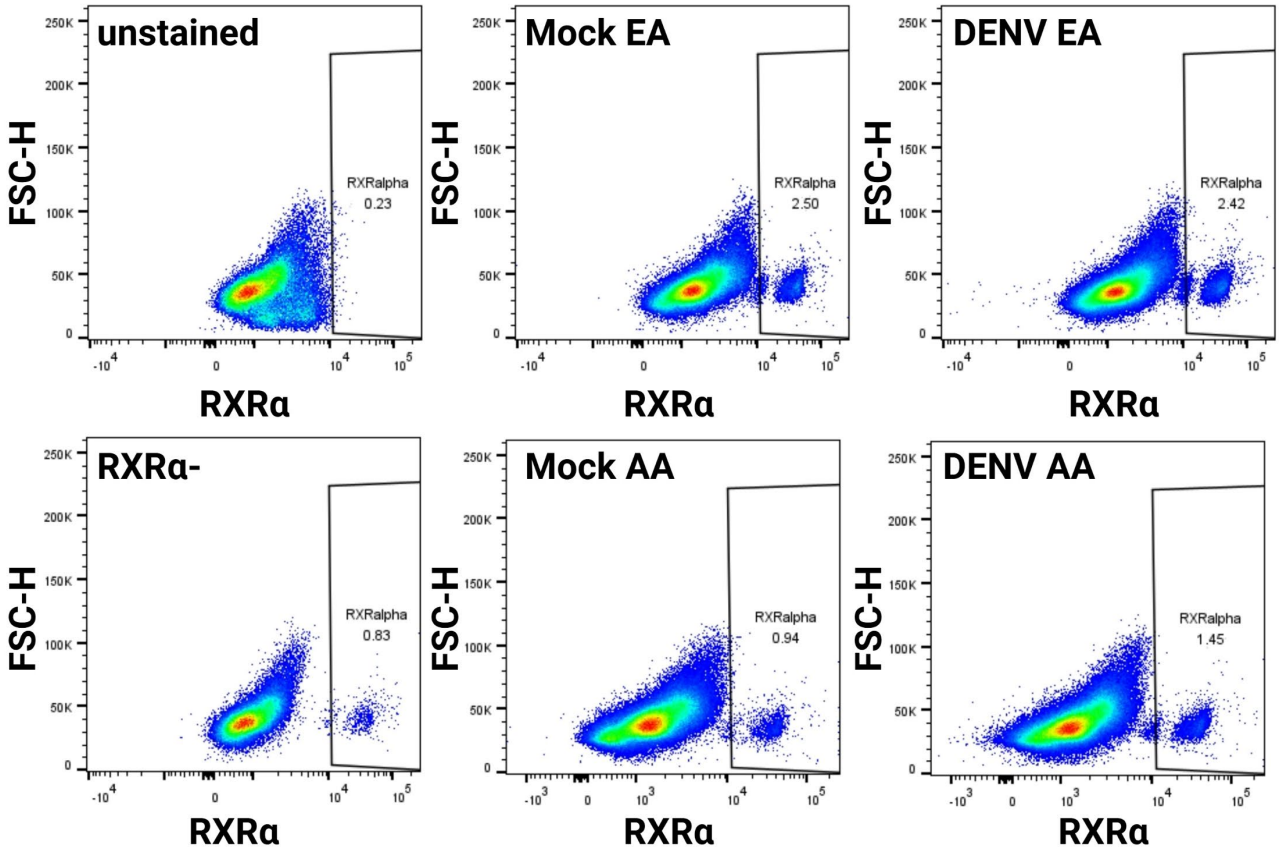

Figure 11. Artifact in RXRα populations with flow cytometry

Layout of epidermal cells stained for RXRα. Events are graphed for an unstained control, a control sample without any RXRα antibody (RXRα-), mock, and infected cells.

Changes in the experiment's design were made to remove the artifact from the population of RXRα. The lasers used to detect the antibodies for DENV and RXRα were noted to be close together, and potential fluorescence spillover from DENV infection was thought to be the cause of the artifact in the RXRα- control. To troubleshoot this, RXRα was stained and analyzed in a separate panel from the DENV antibody. By doing this, the RXRα- control no longer shows a

positive RXRα population (Figure 12A). However, this significantly decreased the amount of RXRα detected in both mock and infected samples (Figure 12A). An average of 1.01% and 1.07% of live cells expressed RXRα in mock and DENV infected EA donors, while 0.39% and 0.54% of live cells in mock and DENV infected AA donors expressed RXRα (Figure 12B). Additional donors are required to further analysis.

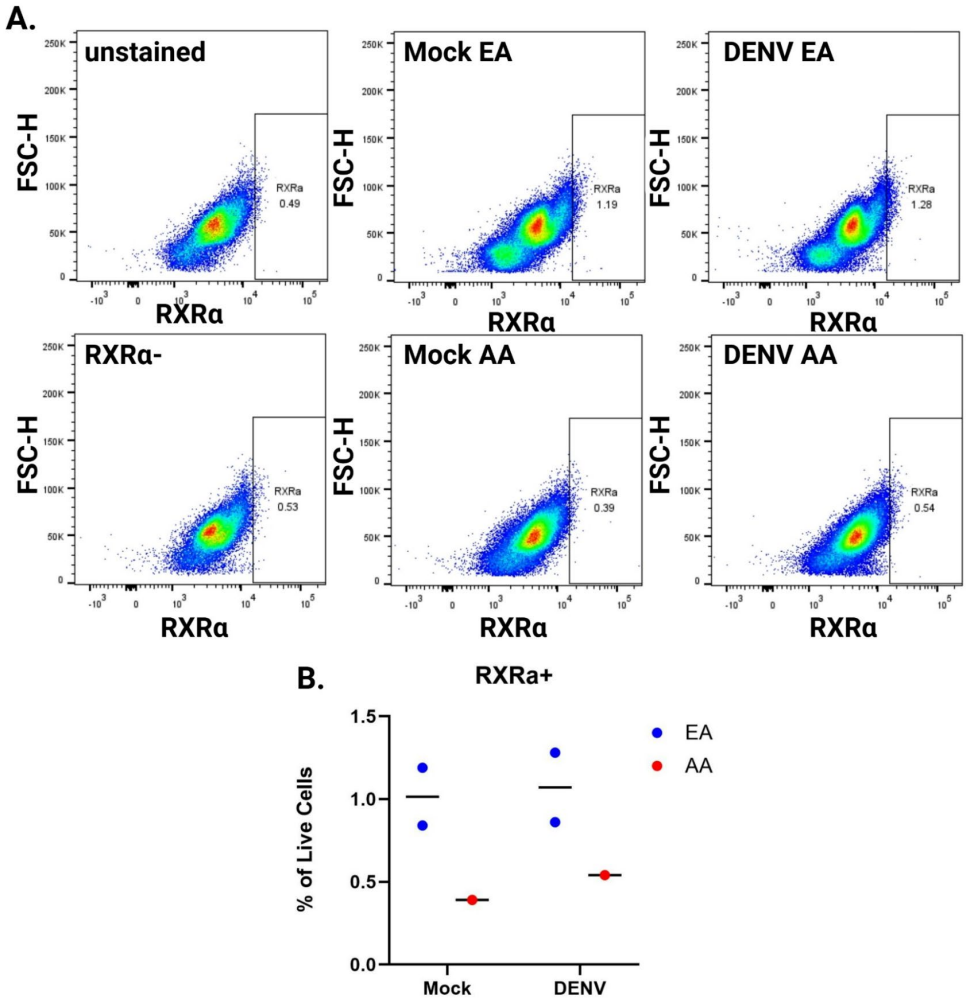

Figure 12. RXRα staining for flow cytometry

Layout of epidermal cells stained for RXRα. Events are graphed for an unstained control, a control sample without any RXRα antibody (RXRα-), mock, and infected cells (A). Percentage of live cells expressing RXRα in mock and DENV infected epidermal cells (n = 3) (B).

4.2 Aim 2: Determine the Epidermal Cells Responsible for Cytokine Production in Response to DENV Infections *in vitro*

4.2.1 Keratinocytes are the Most Abundant Cell Type in the Epidermis

To investigate cell populations within the epidermis, cells were identified with flow cytometry staining by using the following strategy (Figure13). Events were gated by forward scatter area (FSC-A) and forward scatter height (FSC-H) to exclude doublets. Live cells were selected from single cells by gating with V576 and FSC-H. Hematopoietic (CD45+) and non-hematopoietic (CD45-) cells were gated from live cells on a CD45 R718 and FSC-H plot. From the determined CD45- population, keratinocytes were gated on an AE1/AE3 AF488 and FSC-H plot. From the CD45+ gated cells, antigen-presenting cells were selected by HLADR expression on a HLADR RB780 and FSC-H plot. Langerhans cells were selected from HLADR+ cells on a CD1a BV421 and FSC-H plot. Dengue infection was gated from live cells with a YG585 and FSC-H plot.

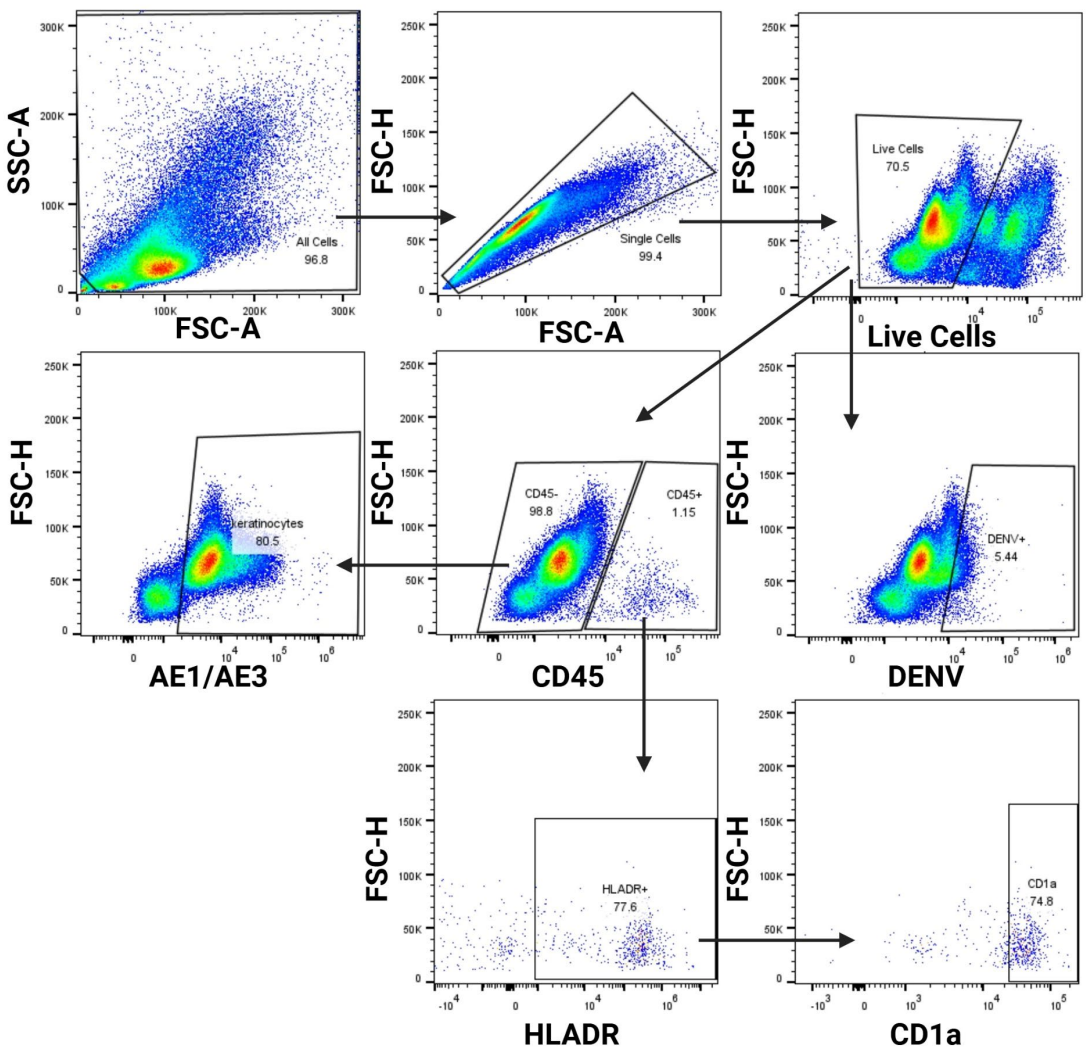

Figure 13. Gating strategy for infected epidermal flow cytometry panel

Following the 24-hour timepoint, mock and DENV infected cells were collected and stained for a panel of epidermal cell markers and anti-dengue virus complex antibody. Of the total number of cells analyzed per condition, the average mock infected sample had 60.6% living cells while an average of 65.9% of cells in DENV infected samples were alive (Figure 14A). This indicates that these samples were relatively viable following tissue processing and infection. Of all of the live cells within each sample, an average of 81.87% of cells were keratinocytes and 1.22% were Langerhans cells (Figure 14B). This was as expected, as literature states that

keratinocytes are the most abundant cell type within the epidermis (sources). Additional donors are required to further analysis.

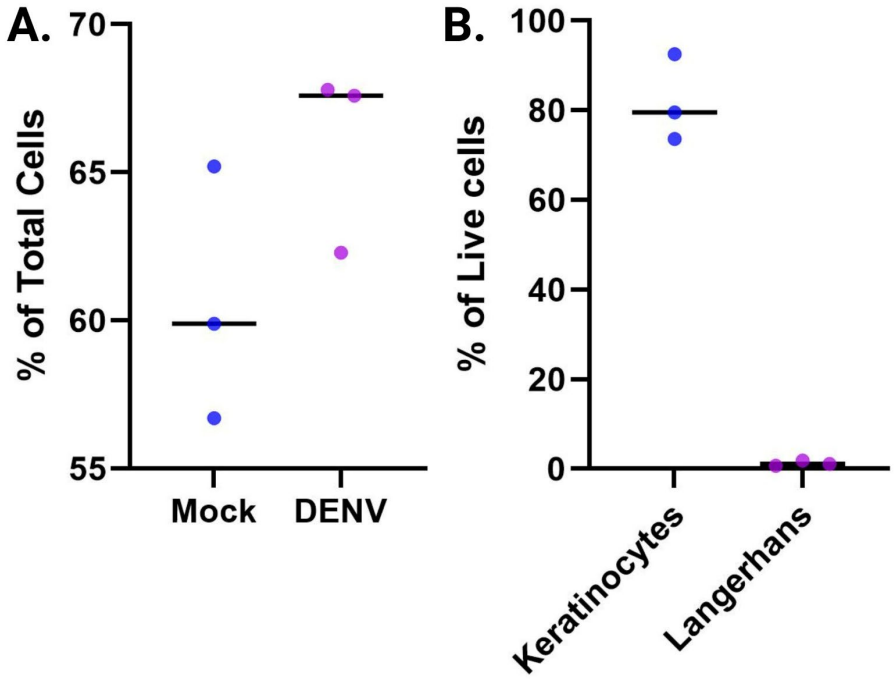

Figure 14. Epidermal cell viability and characterization

The viability of epidermal cells is shown as a percentage of total cells for each donor (A) and distribution of cell types within the epidermis include keratinocytes (AE1/AE3+) and Langerhans (HLADR+ CD1a+) cells (B).

4.2.2 DENV Infection is Greater in European Ancestry Donors

Staining showed that while both EA and AA donors became infected with DENV, there were higher rates of infection in the epidermis of EA donors than AA. EA donors had an infection average of 6.11% in live cells, while only 2.53% of live cells were infected in AA samples (Figure 15A). Infected cells were gated for cell markers AE1/AE3 and HLADR to define the cell types that make up the infected population. In both EA and AA samples, keratinocytes (AE1/AE3+)

were the majority of DENV infected cells (Figure 15B), with a smaller portion of infected cells characterized as antigen-presenting cells (HLADR+) (Figure 15C). In EA donors, around 95.25% of infected cells were keratinocytes while the AA donor had 82.6% keratinocytes. Alternatively, 6.2% of infected cells in the AA donor were antigen-presenting cells, while only 3.1% were antigen-presenting cells in EA donors. Additional donors are required for further analysis.

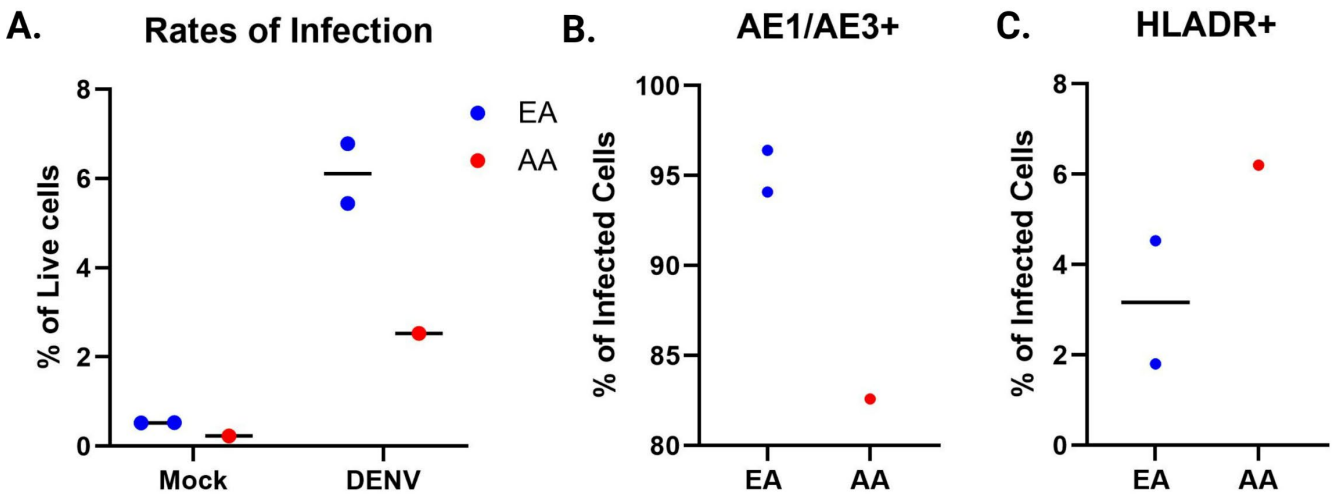

Figure 15. Overall DENV infection rate and infected cell populations

Total DENV infection in the epidermis (A) and percentage of infected cells that are keratinocytes (B) and antigen-presenting cells (C) within European ancestry (EA) and African ancestry (AA) samples (n = 3).

4.2.3 IL-1β and IFN-α Assays are Reproducible

The reproducibility of enzyme-linked immunosorbent assays (ELISAs) is crucial to demonstrate the precision and reliability of the assay. This allows for data comparison across different plates and experiments over time, and indicates that there is consistency in pipetting, dilution of reagents, and washing techniques. Each line represents a standard curve from an experiment conducted on a different date. Overlay of the standard curves for IL-1β (Figure

16A) and IFN-α (Figure 16B) ELISAs show to be consistent across experiments. This demonstrates the reliability and validity of the IL-1β and IFN-α assays and the data that is collected from them.

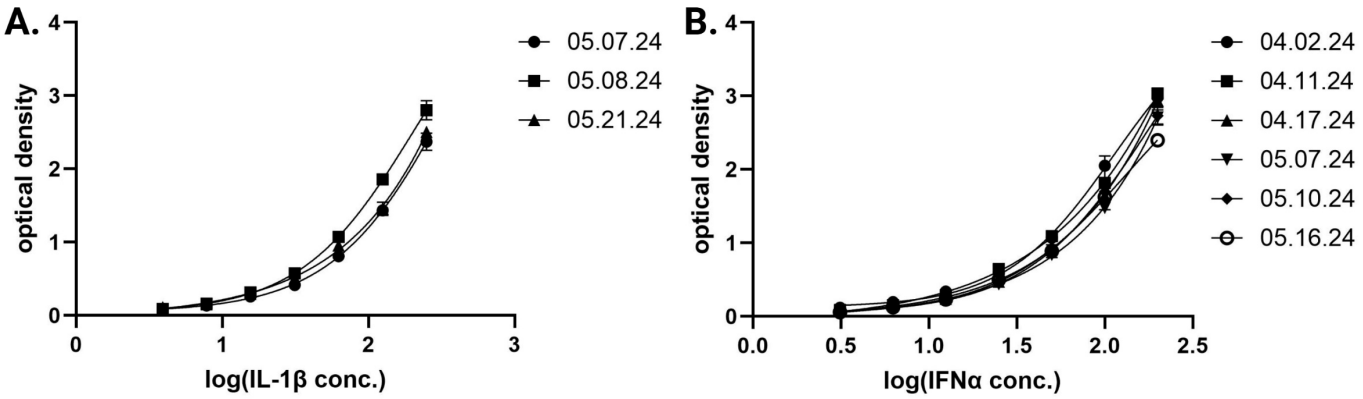

Figure 16. Standard curves demonstrate precision of ELISA kits

Reproducibility of standard curves of IL-1β (A) and IFNα (B) ELISAs from various experiments throughout April and May. The transformed protein concentration (pg/mL) is shown on the x-axis as log(protein concentration) while optical density is graphed on the y-axis.

4.2.4 Secreted IL-1β and IFN-α Concentrations are not Detectable

ELISAs for both IL-1β and IFN-α were performed on cellular supernatants to measure the concentration of cytokines secreted from cells. The initial assays included supernatants collected from $1.5x10^6$ mock and DENV infected cells in a volume of 1.0 mL of media. The optical densities of these samples fell below the lowest concentration on the standard curve, and therefore could not be interpolated. Thinking more cells would produce more cytokines, another assay was run with supernatants collected from $2.0\text{-}2.5x10^6$ cells in a volume of 1.0 mL of media (samples belonging to Michelle Martí). This did not serve as a solution, since the optical densities of these

samples fell outside the standard curve as well. In a final attempt to increase the concentration of cytokines within each sample, $4.0x10^6$ cells were infected and incubated in 500 µL of media. 24 hours post infection, the supernatants were collected and run on an assay. This increased the sample concentration but not enough to fit within the standard curve.

4.2.5 Intracellular IL-1β and IFN-α Concentrations are Unchanged by Dengue Infections

Since cytokine concentration was not detected within in cell supernatants, cell lysates were analyzed to determine if there were any intracellular cytokines that had not been secreted. Three donors of EA were used to compare cytokine production between $1.5\text{-}2.0x10^6$ mock and DENV infected cells. Assays for both IL-1β and IFN-α were run on these samples and their optical densities fell within the standard curve. Cytokine concentrations were interpolated and are shown in Figure 17, with each dot denoting a different donor. While measurable, IL-1β and IFN-α concentrations remained relatively constant between mock and infected lysates in two donors (Figure 17), suggesting that dengue infection does not have an impact on intracellular cytokine production. However, in the third donor, it had an observed increase of IL-1β and decrease of IFNα in DENV infected samples.

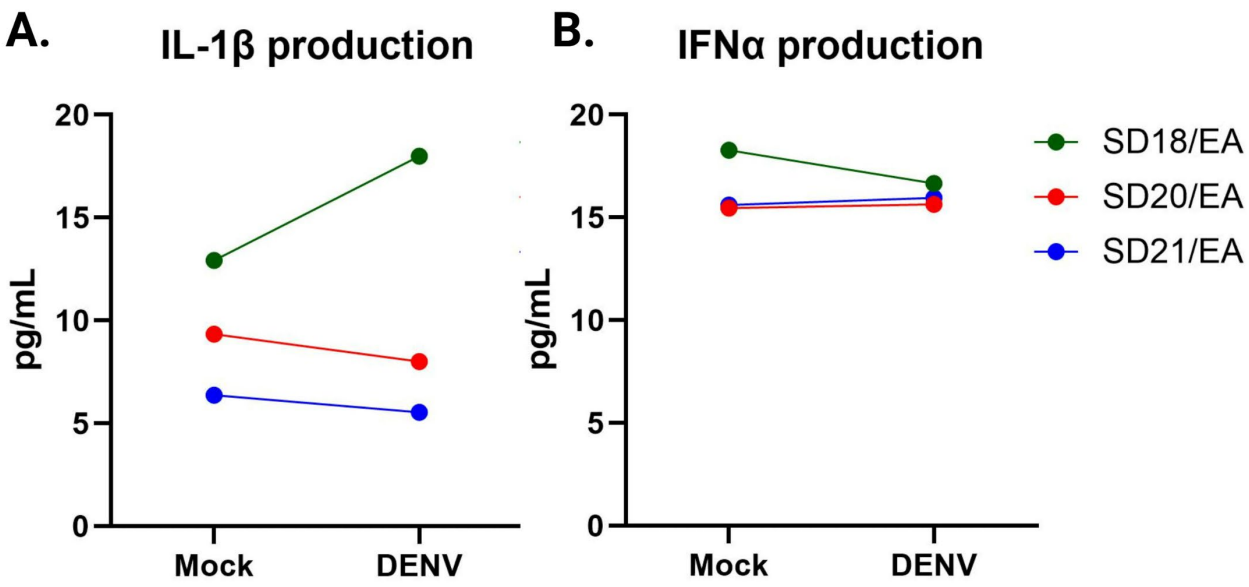

Figure 17. Intracellular IL-1β and IFNα protein concentrations

The measured concentration intracellular IL-1β (A) and IFNα (B) in mock and infected cell lysates from donors of European ancestry (EA) (n = 3). Concentration was determined by ELISA.

5.0 Discussion

RXRα is a nuclear receptor that is ubiquitously expressed in the epidermis, and it primarily functions as a transcription factor to regulate various biological pathways. In viral infections, RXRα has been implicated in having a role in attenuating antiviral immune responses through inhibiting interferon production, as well as inducing proinflammatory responses through the mediation of chemokine expression (37, 42). Studies have demonstrated an association between SNPs of this gene with genetic ancestry and dengue severity (25). The correlation of SNPs in *RXRA* with ancestry could potentially influence the ancestry-related differences in immune responses to dengue infections. The role of RXRα within dengue viral infections is unknown.

The focus of Aim 1 was to investigate the expression of RXRα in human skin in response to dengue viral infection. Chemiluminescent western blotting was utilized to detect the protein in full-thickness and epidermal tissues. In full-thickness tissue, RXRα was detected at the correct molecular weight in both EA and AA samples. Densitometry analysis of the western demonstrated that the expression of RXRα remained relatively high in EA donors before and after DENV infection. However, in AA donors, there was a decrease in RXRα in response to DENV infection. This supports the hypothesis that there is higher expression of RXRα in EA tissue and lower expression within AA tissue in response to DENV infections, which could potentially explain the ancestry-related differences in immune responses. With high expression of RXRα in EA donors, interferon production will be inhibited and thus suppressing antiviral immune responses which correlates with increased susceptibility to viral infections and proinflammatory chemokine production in these donors. Alternatively with low RXRα expression, interferon production is not restricted and is allowed to produce a strong antiviral response, as demonstrated in donors of AA.

Western blots with epidermal cell lysates did not reproduce the same conclusions as those from full-thickness tissue. Quantification of these membranes showed no difference in RXRα expression between EA and AA donors across all infection timepoints, which contradicts the hypothesis of the aim. The differences between protein expression in the western blots could potentially be due to RXRα expression within the dermis layer of full-thickness tissue that is not accounted for within the epidermal samples. Western blots on dermal cell lysates should be conducted to examine RXRα within this skin layer. Antibody staining for flow cytometry was additionally used to try to measure RXRα within epidermal cells, but very little protein was detected by this methodology. Comparing results of western blots and flow cytometry between donors demonstrates inconsistencies of protein expression. Further optimization of the antibody panel used for flow cytometry is required for better detection of RXRα.

One of the optimizations made to the western blot protocol involved normalizing glyceraldehyde-3-phosphate dehydrogenase (GAPDH) protein expression between samples. This was to resolve issues with the loading control, as there was inconsistent protein expression across wells. GAPDH was chosen as a loading control as it is a housekeeping protein involved in glycolysis and should be abundantly expressed within all cells, and it has a lower molecular weight than RXRα that allows simultaneous detection on western blots. A possible explanation for the inconsistencies in GAPDH expression is that the glycolysis pathway is affected by several viral glycoproteins during dengue infections (43, 44), including a decrease in glycolytic activity during DENV-2 infections (45). To further investigate RXRα using western blots, a different housekeeping protein should be used as a loading control to affirm the results within Aim 1. Vinculin would be a possible protein, as it has a higher molecular weight than RXRα.

The purpose of Aim 2 was to examine cytokine producing cells within the epidermis during dengue infection. Using flow cytometry, keratinocytes were identified as the most prevalent cell type within the epidermis, as commonly discussed in literature (13, 14), with a smaller subset of cells identified as Langerhans cells. EA donors show higher infection rates than donors of AA, which is consistent with the lab's prior immunofluorescence data. Keratinocytes make up the majority of infected cells within the epidermis, with some infection in antigen-presenting cells as well. This reinforces that keratinocytes are the earliest and most common targets of viral infection, as they are highly susceptible to DENV (13, 14). Other members in the lab have conducted similar experiments with greater statistical power and they have observed similar trends in their data. Despite the lack of statistical power in my experiments, this suggests that my results are true. More donors are required to provide statistical significance of these results.

Cytokine production in epidermal cells 24-hours post DENV infection were examined with enzyme-linked immunosorbent assays (ELISAs). Secreted interleukin-1β (IL-1β) and interferon-α (IFNα) could not be measured in either mock or DENV infected cell supernatants. A possible explanation for this would be that the supernatants were too diluted and required further concentration for detection on the assays. Attempts were made to increase cytokine concentration within the supernatants, but none were successful. IL-1β and IFNα concentrations were detected and measured in epidermal cell lysates, however, giving insight into the accumulation of intracellular cytokines. Following 24-hours post-infection, there were no differences in cytokine concentrations of mock and infected cells in both IL-1β and IFNα assays. Cytokines are proteins produced to influence nearby immune cells to mediate inflammatory and antiviral mechanisms in the case of IL-1β and IFNα, respectively. As part of the innate immune response, cytokines are produced hours after infection. One study showed a significant increase in IFNα production as

soon as 2-hours post DENV infection in human skin but returned to baseline levels around 12-hours post infection (13). The 24-hour timepoint may be too long after infection to detect any differences in cytokine concentrations between mock and infected samples, however, earlier timepoints may provide a more comprehensive insight on cytokine production within cells.

Results from this study were limited by access and availability of tissue donors, as the majority of experiments only included data from three donors (n = 3). Tissues are received on a random basis, and experiments rely on the hospital's surgery schedule. Tissue availability is impacted by cancellation of surgeries, the size of tissue removed/collected, and requests of tissue from other collaborating laboratories. Surgeries involving AA donors are less common than EA donors, so these tissues are received on a more infrequent basis. A lot of optimizations were involved in this project for all experiments, and this required a significant amount of time to complete. Once the methodologies were optimized and capable of producing reliable results, there was not enough time to compile data from a significant number of donors. Consequently, more donors will be required to support the findings within this study.

Knowledge regarding the role of RXRα in dengue viral infections remains incomplete. Additionally, Aim 2 remains an open question that will require further investigation to answer, as the epidermal cell types responsible for producing IL-1β and IFNα in dengue infections was not elucidated by this project. This project should be continued in the future, as it could provide beneficial insight on what drives ancestry-related differences in dengue viral infections. RXRα may play a role in the relationship between genetic ancestry and severe dengue, but without further research, this will remain unknown.

In conclusion, the majority of people in the world live within areas at risk of dengue infections (3), and there are several host factors that leave some individuals more vulnerable and

susceptible to disease than others. Ancestry has been implicated as a potential risk factor for severe dengue, suggesting that individuals of African ancestry have conferred protection while those of European ancestry are more susceptible to infection. Preliminary data from our lab's *ex vivo* human skin model begins to describe ancestry-related differences in the early innate immune response to dengue viral infections. By understanding genetic and immunological influences on viral pathogenesis, we can better comprehend the host response to viral infections and begin to explain why certain populations are more susceptible to disease. If we can understand what protects individuals of African ancestry from severe dengue, we could potentially develop interventions that can protect more susceptible biogeographical populations in the world. This would allow for more effective and targeted approaches that would ultimately improve patient health outcomes, prevent the spread of disease, and reduce the risk of infection within vulnerable communities.

6.0 Future Directions

Many questions remain following this project, which can be addressed by future studies. Some experiments that could improve upon the results from this project includes:

1. Detect RXRα expression in dermal cell lysates using chemiluminescent western blots.
2. Repeat the same flow cytometry experiments in Aim 1 with more donors to add statistical power to current results.
3. Optimize the panel of antibodies for flow cytometry in Aim 1 to identify RXRα expression and which cells are responsible for producing the protein.
3. Repeat the same flow cytometry experiments in Aim 2 with more donors to add statistical power to current results.
4. Incorporate intracellular cytokine staining to the flow cytometry panel used in Aim 2 to examine which cells are responsible for cytokine production.
5. Repeat ELISAs using cellular lysates from more donors to add statistical power to current results.
6. Measure the concentrations of IL-1β and IFNα at earlier timepoints (ex. 0-hours, 3-hours, 6-hours, and 12-hours post DENV infection) in mock and infected epidermal cell lysates and supernatants.

Using the lab's human skin model, the early immune response to dengue viral infections can be studied. This model provides opportunities to explore viral pathogenesis and the production of the immune response to dengue. By implementing these future directions, the shortcomings of this project can be addressed and provide further insights to potentially explain the ancestry-related differences in immune responses to dengue infection.

7.0 Public Health Significance

Dengue is the most prevalent arboviral infection in the world. It is endemic in over 100 countries, and more than half of the world's population live at risk for infection with up to 400 million infections per year (3). Around 100 million of these infections develop symptoms, which are usually mild, febrile illnesses (3). Severe dengue is more likely to develop from secondary infections with more severe health complications that can ultimately be fatal (46). Currently, there are no antiviral drugs available for these infections and the only treatment options include medication to alleviate pain and supportive care for extreme complications due to severe dengue (47). There are two vaccines undergoing late-stage development (QDenga and T003/T005) and one that is currently licensed (Dengvaxia) (47, 48). However, Dengvaxia has been shown to put seronegative recipients at higher risk of developing severe dengue in subsequent infections (48). By studying the immune response to viral infections and understanding viral pathogenesis, therapeutic developments can be made to mitigate the impact dengue has on global health. These studies would provide a better understanding of host-viral interactions that can identify anti-viral drug targets and help improve vaccine safety, effectiveness, and development.

Bibliography

1. Guzman MG, Harris E. 2015. Dengue. The Lancet 385:453–465.

2. Guzman MG, Gubler DJ, Izquierdo A, Martinez E, Halstead SB. 2016. Dengue infection. Nat Rev Dis Primers 2:16055.

3. Bhatt S, Gething PW, Brady OJ, Messina JP, Farlow AW, Moyes CL, Drake JM, Brownstein JS, Hoen AG, Sankoh O, Myers MF, George DB, Jaenisch T, Wint GRW, Simmons CP, Scott TW, Farrar JJ, Hay SI. 2013. The global distribution and burden of dengue. Nature 496:504–507.

4. Murphy BR, Whitehead SS. 2011. Immune Response to Dengue Virus and Prospects for a Vaccine. Annu Rev Immunol 29:587–619.

5. Kraemer MUG, Sinka ME, Duda KA, Mylne AQN, Shearer FM, Barker CM, Moore CG, Carvalho RG, Coelho GE, Van Bortel W, Hendrickx G, Schaffner F, Elyazar IRF, Teng H-J, Brady OJ, Messina JP, Pigott DM, Scott TW, Smith DL, Wint GRW, Golding N, Hay SI. 2015. The global distribution of the arbovirus vectors Aedes aegypti and Ae. albopictus. Elife 4:e08347.

6. Lwande OW, Obanda V, Lindström A, Ahlm C, Evander M, Näslund J, Bucht G. 2020. Globe-Trotting Aedes aegypti and Aedes albopictus: Risk Factors for Arbovirus Pandemics. Vector Borne Zoonotic Dis 20:71–81.

7. Rezza G. 2012. Aedes albopictus and the reemergence of Dengue. BMC Public Health 12:72.

8. Leandro AS, Chiba De Castro WA, Garey MV, Maciel-de-Freitas R. 2024. Spatial analysis of dengue transmission in an endemic city in Brazil reveals high spatial structuring on local dengue transmission dynamics. Sci Rep 14:8930.

9. Shepard DS, Coudeville L, Halasa YA, Zambrano B, Dayan GH. 2011. Economic impact of dengue illness in the Americas. Am J Trop Med Hyg 84:200–207.

10. Shepard DS, Undurraga EA, Halasa YA. 2013. Economic and Disease Burden of Dengue in Southeast Asia. PLoS Negl Trop Dis 7:e2055.

11. Ennaji MM. 2020. Emerging and reemerging viral pathogens. Academic press, an imprint of Elsevier, London.

12. World Health Organization. 2009. Dengue guidelines for diagnosis, treatment, prevention and control : new edition.

13. Duangkhae P, Erdos G, Ryman KD, Watkins SC, Falo LD, Marques ETA, Barratt-Boyes SM. 2018. Interplay between Keratinocytes and Myeloid Cells Drives Dengue Virus Spread in Human Skin. Journal of Investigative Dermatology 138:618–626.

14. Martí MM, Castanha PMS, Barratt-Boyes SM. 2024. The Dynamic Relationship between Dengue Virus and the Human Cutaneous Innate Immune Response. Viruses 16:727.

15. Van Seventer JM, Hochberg NS. 2017. Principles of Infectious Diseases: Transmission, Diagnosis, Prevention, and Control, p. 22–39. *In* International Encyclopedia of Public Health. Elsevier.

16. Yuan K, Chen Y, Zhong M, Lin Y, Liu L. 2022. Risk and predictive factors for severe dengue infection: A systematic review and meta-analysis. PLoS One 17:e0267186.

17. National Institutes of Health (US). 2007. Biological Sciences Curriculum Study: NIH Curriculum Supplement Series. National Institutes of Health (US). https://www.ncbi.nlm.nih.gov/books/NBK20363/.

18. Brookes AJ. 1999. The essence of SNPs. Gene 234:177–186.

19. Sauna ZE, Kimchi-Sarfaty C. 2011. Understanding the contribution of synonymous mutations to human disease. Nat Rev Genet 12:683–691.

20. Trejo-de La O A, Hernández-Sancén P, Maldonado-Bernal C. 2014. Relevance of single-nucleotide polymorphisms in human TLR genes to infectious and inflammatory diseases and cancer. Genes Immun 15:199–209.

21. Kosoy R, Nassir R, Tian C, White PA, Butler LM, Silva G, Kittles R, Alarcon-Riquelme ME, Gregersen PK, Belmont JW, De La Vega FM, Seldin MF. 2009. Ancestry informative marker sets for determining continental origin and admixture proportions in common populations in America. Hum Mutat 30:69–78.

22. Padakanti S, Tiong K-L, Chen Y-B, Yeang C-H. 2021. Genotypes of informative loci from 1000 Genomes data allude evolution and mixing of human populations. Sci Rep 11:17741.

23. Wang L-J, Zhang CW, Su SC, Chen H-IH, Chiu Y-C, Lai Z, Bouamar H, Ramirez AG, Cigarroa FG, Sun L-Z, Chen Y. 2019. An ancestry informative marker panel design for individual ancestry estimation of Hispanic population using whole exome sequencing data. BMC Genomics 20:1007.

24. Sierra BDLC, Kourí G, Guzmán MG. 2007. Race: a risk factor for dengue hemorrhagic fever. Arch Virol 152:533–542.

25. Sierra B, Triska P, Soares P, Garcia G, Perez AB, Aguirre E, Oliveira M, Cavadas B, Regnault B, Alvarez M, Ruiz D, Samuels DC, Sakuntabhai A, Pereira L, Guzman MG. 2017. OSBPL10, RXRA and lipid metabolism confer African-ancestry protection against dengue haemorrhagic fever in admixed Cubans. PLoS Pathog 13:e1006220.

26. Chacón-Duque JC, Adhikari K, Avendaño E, Campo O, Ramirez R, Rojas W, Ruiz-Linares A, Restrepo BN, Bedoya G. 2014. African genetic ancestry is associated with a protective effect on Dengue severity in colombian populations. Infect Genet Evol 27:89–95.

27. Boillat-Blanco N, Klaassen B, Mbarack Z, Samaka J, Mlaganile T, Masimba J, Franco Narvaez L, Mamin A, Genton B, Kaiser L, D'Acremont V. 2018. Dengue fever in Dar es Salaam, Tanzania: clinical features and outcome in populations of black and non-black racial category. BMC Infect Dis 18:644.

28. Cano-Gamez E, Trynka G. 2020. From GWAS to Function: Using Functional Genomics to Identify the Mechanisms Underlying Complex Diseases. Front Genet 11:424.

29. Dawson MI, Xia Z. 2012. The retinoid X receptors and their ligands. Biochim Biophys Acta 1821:21–56.

30. Zhang X, Su Y, Chen L, Chen F, Liu J, Zhou H. 2015. Regulation of the nongenomic actions of retinoid X receptor-α by targeting the coregulator-binding sites. Acta Pharmacol Sin 36:102–112.

31. Chen L, Wu L, Zhu L, Zhao Y. 2018. Overview of the structure-based non-genomic effects of the nuclear receptor RXRα. Cell Mol Biol Lett 23:36.

32. Szanto A, Narkar V, Shen Q, Uray IP, Davies PJA, Nagy L. 2004. Retinoid X receptors: X-ploring their (patho)physiological functions. Cell Death Differ 11:S126–S143.

33. Liby KT, Sporn MB. 2016. Rexinoids for prevention and treatment of cancer: opportunities and challenges. Curr Top Med Chem.

34. Lin X-F, Zhao B-X, Chen H-Z, Ye X-F, Yang C-Y, Zhou H-Y, Zhang M-Q, Lin S-C, Wu Q. 2004. RXRα acts as a carrier for TR3 nuclear export in a 9-cis retinoic acid-dependent manner in gastric cancer cells. Journal of Cell Science 117:5609–5621.

35. Zhang X, Zhou H, Su Y. 2016. Targeting truncated RXRα for cancer therapy. Acta Biochim Biophys Sin (Shanghai) 48:49–59.

36. Shen Q, Bai Y, Chang KCN, Wang Y, Burris TP, Freedman LP, Thompson CC, Nagpal S. 2011. Liver X receptor-retinoid X receptor (LXR-RXR) heterodimer cistrome reveals coordination of LXR and AP1 signaling in keratinocytes. J Biol Chem 286:14554–14563.

37. Núñez V, Alameda D, Rico D, Mota R, Gonzalo P, Cedenilla M, Fischer T, Boscá L, Glass CK, Arroyo AG, Ricote M. 2010. Retinoid X receptor alpha controls innate inflammatory responses through the up-regulation of chemokine expression. Proc Natl Acad Sci U S A 107:10626–10631.

38. Li M, Indra AK, Warot X, Brocard J, Messaddeq N, Kato S, Metzger D, Chambon P. 2000. Skin abnormalities generated by temporally controlled RXRα mutations in mouse epidermis. Nature 407:633–636.

39. Li M, Messaddeq N, Teletin M, Pasquali J-L, Metzger D, Chambon P. 2005. Retinoid X receptor ablation in adult mouse keratinocytes generates an atopic dermatitis triggered by thymic stromal lymphopoietin. Proc Natl Acad Sci USA 102:14795–14800.

40. Rőszer T, Menéndez-Gutiérrez MP, Cedenilla M, Ricote M. 2013. Retinoid X receptors in macrophage biology. Trends in Endocrinology & Metabolism 24:460–468.

41. Leopold Wager CM, Arnett E, Schlesinger LS. 2019. Macrophage nuclear receptors: Emerging key players in infectious diseases. PLoS Pathog 15:e1007585.

42. Ma F, Liu S-Y, Razani B, Arora N, Li B, Kagechika H, Tontonoz P, Núñez V, Ricote M, Cheng G. 2014. Retinoid X receptor α attenuates host antiviral response by suppressing type I interferon. Nat Commun 5:5494.

43. Silva EM, Conde JN, Allonso D, Ventura GT, Coelho DR, Carneiro PH, Silva ML, Paes MV, Rabelo K, Weissmuller G, Bisch PM, Mohana-Borges R. 2019. Dengue virus nonstructural 3 protein interacts directly with human glyceraldehyde-3-phosphate dehydrogenase (GAPDH) and reduces its glycolytic activity. Sci Rep 9:2651.

44. Allonso D, Andrade IS, Conde JN, Coelho DR, Rocha DCP, da Silva ML, Ventura GT, Silva EM, Mohana-Borges R. 2015. Dengue Virus NS1 Protein Modulates Cellular Energy Metabolism by Increasing Glyceraldehyde-3-Phosphate Dehydrogenase Activity. J Virol 89:11871–11883.

45. Chumchanchira C, Ramphan S, Sornjai W, Roytrakul S, Lithanatudom P, Smith DR. 2024. Glycolysis is reduced in dengue virus 2 infected liver cells. Sci Rep 14:8355.

46. Kalayanarooj S. 2011. Clinical Manifestations and Management of Dengue/DHF/DSS. Trop Med Health 39:83–87.

47. Tayal A, Kabra SK, Lodha R. 2023. Management of Dengue: An Updated Review. Indian J Pediatr 90:168–177.

48. Wilder-Smith A. 2020. Dengue vaccine development: status and future. Bundesgesundheitsblatt Gesundheitsforschung Gesundheitsschutz 63:40–44.